QMetro++ - Python optimization package for large scale quantum metrology with customized strategy structures

Piotr Dulian^{1,2}, Stanisław Kurdziałek², and Rafał Demkowicz-Dobrzański²

QMetro++ is a Python package containing a set of tools dedicated to identifying optimal estimation protocols that maximize quantum Fisher information Optimization can be performed for an arbitrary arrangement of input parameter encoding channels, states, noise correlations, control operations and measurements. The use of tensor networks and iterative see-saw algorithm allows for an efficient optimization even in the regime of large number of channel uses $(N \approx 100)$. Additionally, the package comes with an implementation of the recently developed methods for computing fundamental upper bounds on QFI, which serve as benchmarks of optimality of the outcomes of numerical optimization. All functionalities are wrapped up in a userfriendly interface which enables defining strategies at various levels of detail.

Link: https://github.com/pdulian/qmetro

1 Introduction

Quantum metrology [1–4] is now rightfully regarded as one of the main pillars of rapidly developing field of quantum technologies [5]. It focuses on the ways to exploit delicate quantum features of light and matter to enhance the sensitivity of practical measuring devices. Apart from numerous experimental breakthroughs in the field, including the use of squeezed states of light in gravitational wave detectors [6, 7], quantum enhanced magnetometry [8], gravitometry [9], atomic clocks [10] and many others, the field has also enjoyed significant theoretical progress with numerous analytical and numeri-

cal methods being developed, that help to design better metrological protocols as well as understand the fundamental limitations of quantum-enhanced protocols in the presence of decoherence [11–23].

The purpose of this package is to make these advanced and powerful numerical methods accessible to the community. We realize that despite the fact that the core elements of the methods have been discussed in the literature for a couple of years already, they are still not widely used in the field due to their somewhat steep 'initial learning curve' and the fact that there is no single publication that provides a unified presentation of all of them, not to mention a numerical package. Moreover, we significantly expand the applicability of the latest tensor network-based methods to include general protocol structures, which allows to deal with e.g. collisional metrological schemes.

Not so rarely, we have come across research conducted in the field, where the problem of optimization of quantum metrological protocols has been approached using general-purpose optimization tools (including even the latest AI methods), which in the end did not result in a particular efficient numerical algorithm, the results of numerical optimization had not optimality guarantee and were not benchmarked with known fundamental precision bounds [citations intentionally hidden here!].

This package adopts the frequentist approach to quantum metrology and focuses on quantum Fisher information (QFI) as the figure-of-merit to be optimized [24–26]. At this point, we do not include quantum Bayesian methods in the package, even though some of the optimization procedure discussed here have their Bayesian counterparts, and may be added in the future updates. The

¹Centre for Quantum Optical Technologies, Centre of New Technologies, University of Warsaw, Banacha 2c, 02-097 Warszawa, Poland

²Faculty of Physics, University of Warsaw, Pasteura 5, 02-093 Warszawa, Poland

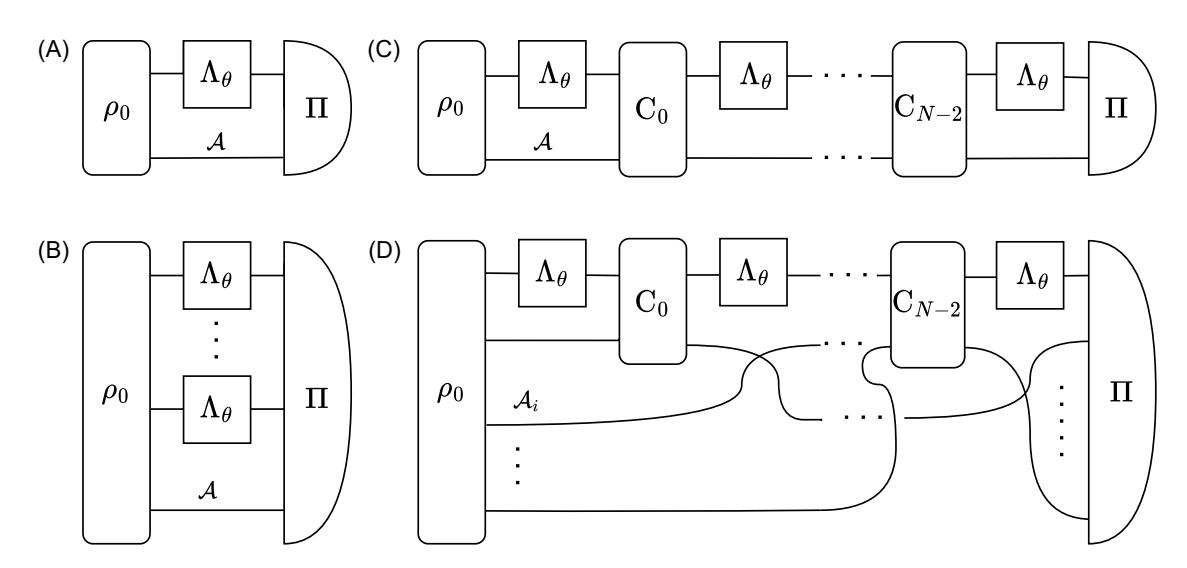


Figure 1: Different classes of metrological strategies that one can optimize using the package: (A) optimization of a single channel input probe ρ_0 (potentially entangled with an ancillary system \mathcal{A}), (B) optimization of an entangled state ρ_0 of N input probes in a parallel strategy (potentially additionally entangled with an ancillary system \mathcal{A}), (C) optimization of an input probe ρ_0 and control operations C_i in an adaptive metrological scheme, (D) a customized protocol structure, here inspired by quantum collisional models, where multi-partite entangled ancillary state is sent piece-by-piece to interact with a common sensing system via interaction gates C_i . Here the optimization may affect either the input state ρ_0 or interaction gates C_i or both. The above strategies correspond to functions listed in Table 1.

strategy		package functions	section
(A) single channel		mop_channel_qfi, iss_channel_qfi	3.2
(B) parallel	small N	<pre>mop_parallel_qfi, iss_parallel_qfi</pre>	
	large N	iss_tnet_parallel_qfi	3.3
	bound	par_bounds	
	small N	<pre>mop_parallel_qfi, iss_parallel_qfi</pre>	
(C)	large N	iss_tnet_adaptive_qfi	3.4
adaptive	bound	ad_bounds	3.5
	corr. noise bound	${\tt ad_bounds_correlated}$	
(D) customized		$iss_opt + \dots$	4

Table 1: An overview of package functions that allow to identify the optimal metrological strategies with a particular protocol structure. Examples of a particular protocol structure optimization, with complete Python codes, are provided in the sections listed in the last column. The corresponding structures are depicted in Fig. 1.

main reason is that, from our numerical experience, the Bayesian approach does not combine well with the tensor-network optimization procedures, and hence cannot be efficiently used to study the performance of protocols in the large number of channel uses, see more discussion in the conclusion section.

The crucial and unique feature of our package is the ability to go to large scale metrological problems, involving multiple-channel uses, whether in adaptive sequential schemes, parallel schemes, or any conceivable protocol struc-

ture one may think of, and optimize the protocols without any prior assumption regarding the class of operations allowed, apart from the restriction on the dimensionality of the physical and ancillary spaces involved, see Fig. 1.

As such, our package completely supersedes the TNQMetro package [27], which was designed to deal with optimization of input probes in parallel metrological scheme involving large number of channels. Compared with the previous package, the new one not only allows for a full flexibility of choosing the protocol structure one wants

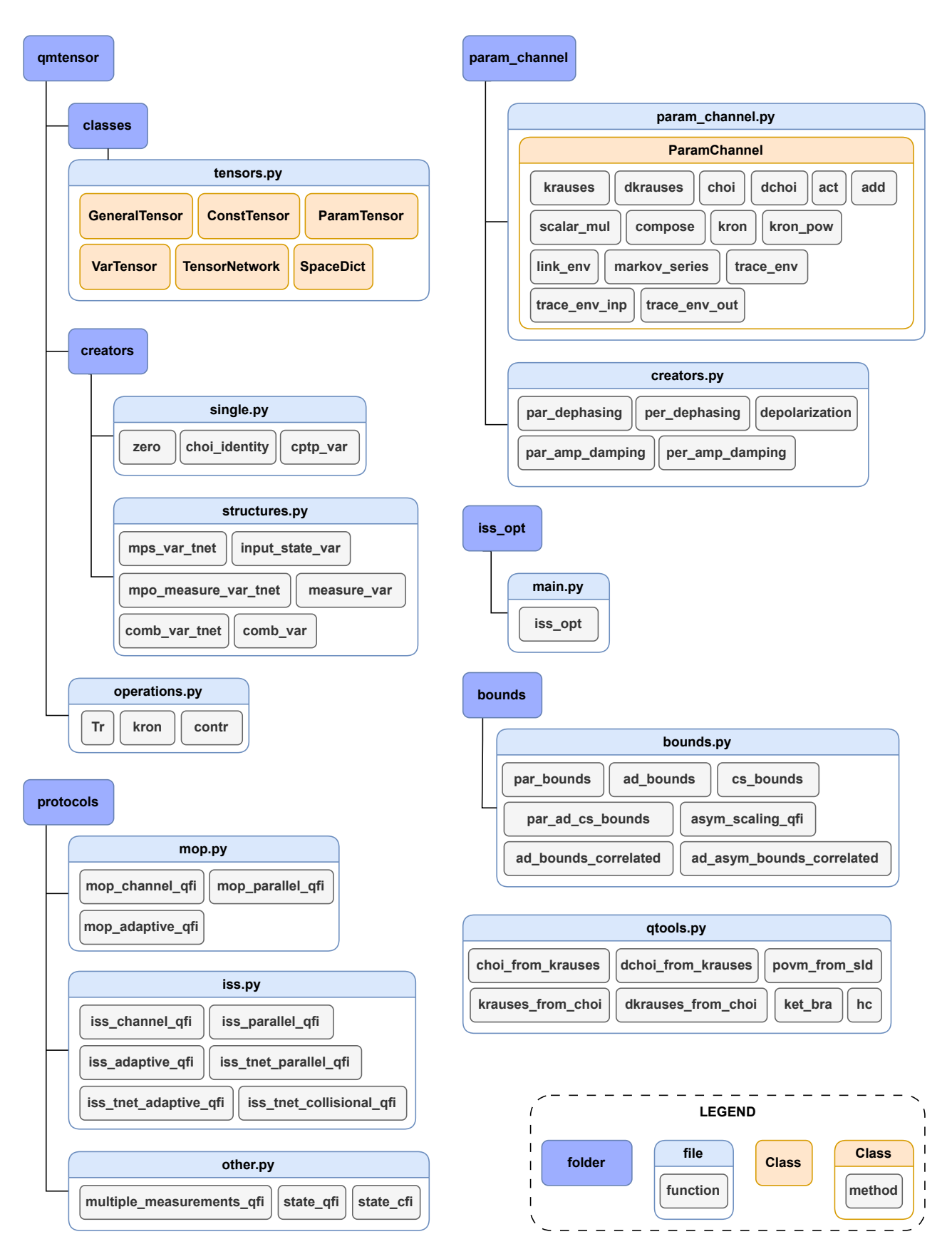


Figure 2: File structure of the package. Classes from tensors.py file are displayed in more detail in Fig. 10.

to analyze, but even in the basic parallel channels scenario offers a significantly improved userfriendly interface that allows to deal with large class of problems, including correlated noise models, in a straightforward way.

The second unique component of the package is the implementation of the methods that compute fundamental metrological bounds in a very efficient way. These bounds are the tightest universal bounds known in the literature [21] and include the very latest method to compute bounds in case of *correlated* noise models as well [28]! The bounds may serve as benchmarks for the protocols found as a result of numerical optimization.

Interestingly, in case of uncorrelated noise models, it is known that the bounds are tight in the asymptotic limit of large number of channel uses [18, 21]. This fact makes the bounds doubly-powerful. Not only do they serve as a proof that a given protocol is optimal, if it saturates the bound, but also indicate that the protocol is in fact not optimal if one sees a persistent gap between the performance of the numerically found protocol and the bound that does not diminish with the increase of the number of channels used.

The main functionalities of the package are summarized in Table 1, where we indicate the methods designed to optimize the strategies corresponding to the structures depicted in Fig. 1, including single-channel strategy (A), parallel channels strategy (B), adaptive strategy (C) and customized strategy (D).

In the small-N regime, protocols (A), (B) and (C) may be optimized as a whole, without the use of tensor-network structures. This allows us to perform the optimization using two alternative approaches: the iterative see-saw (ISS) and the minimization over purifications (MOP).

The MOP approach has the advantage over ISS that the numerical solution found is guaranteed to be optimal, see Sec. 2.3. Hence, this is the method to be chosen for small-scale problems, where Hilbert spaces dimensions are reasonably small. However, MOP methods cannot be generalized to large-scale problems and combined with tensor-network framework—then, one needs to resort to the ISS approach. The ISS has no guarantee to converge to the true optimal solution, but is constructed in a way that every iteration step cannot reduce the optimized figure-of-merit,

see Sec. 2.4.

The main advantage of ISS over MOP is that it naturally combines with tensor-network formalism and may work in the large-N regime. In this case the optimization is performed over each local node in the tensor-network structure separately, whether it represents a part of the input state, control operation or measurement. For this approach one may use the higher-level functions, iss_tnet_parallel_qfi or iss_tnet_adaptive_qfi, dedicated to optimizing standard protocols structures such as parallel (B) or adaptive (C) ones respectively. Alternatively, one can construct a customized structure of the protocol, and use a lower level function iss_opt which performs the iss optimization for arbitrary tensor-network structure, see Sec. 4 for a detailed example.

Finally, the package comes with a number of functions that allow to compute fundamental bounds given just the structure of an individual parameter-encoding quantum channel. The two functions, par_bounds and ad_bounds allow to compute the bounds in case of uncorrelated noise models valid for parallel and adaptive strategies. These bounds are known to be asymptotically saturable for $N \to \infty$, see Sec. 2.5. The function ad_bounds_correlated, on the other hand, provides bounds in case of correlated noise models, where there is some quantum environment that connects different instances of channels action, and captures the effects of e.g. non-Markovianity. This function provides valid bounds which may be tightened at the expense of numerical complexity, but unlike uncorrelated noise bounds, they are not guaranteed to be tight.

The detailed structure of the package is depicted in Fig. 2. The higher-level optimization functions are collected in the protocols folder, including both MOP and ISS protocols, with the latter one both in the standard as well as tensor-network variant (tnet). folder also provides a couple of auxiliary functions: a function for computation of QFI of a state (state_qfi), a function for computation of classical Fisher information given a state and measurement (state_cfi) and a function multiple_measurements_qfi that calculates the optimal distribution of N channels into k experiments with N_i ($N = \sum_{i=1}^k N_i$) channels. The functions computing bounds are gathered in the bounds folder, where apart from the standard procedure to compute the bounds for finite number of channel uses, there are also asymptotic variants that compute the bounds in the asymptotic limit $N \to \infty$.

As a bonus feature, we have also included bounds that are valid even in the more general than adaptive causal superpositions strategies (cs), see [21]. They are, however, not the essential element of the package, since they do not have a counterpart large-scale optimization procedure to find the optimal protocols, as tensornetwork formalism is not obviously compatible with this framework.

In order to perform the optimization using higher-level functions or compute the bounds, one needs to specify the form of the parameter dependent channel Λ_{θ} . The param_channel folder contains all the necessary methods to construct the channel and includes also some exemplary predefined channels in the creators.py file. The channel may be provided in a number of different ways: either through a list of Kraus operatos, or a CJ matrix, or finally as a time integrated quantum Master equation, see Sec. 3.2.

In order to perform optimization of protocols with customized structures one needs to resort to low-level ISS optimization function <code>iss_opt</code> and construct the desired protocol structure using the classes provided in <code>tensors.py</code> file, which allow to specify the elements of the protocol that will be optimized (<code>VarTensor</code>), elements that are fixed (<code>ConstTensor</code>) and elements that include parameter to be estimated (<code>ParamTensor</code>), see Sec. 4.

The package comes also with a number of useful auxiliary functions, combined in qtools.py and other.py, details can be found in the documentation of the package [29]

This paper is organized as follows. In Sec. 2 we provide a theoretical background for the essential quantum metrological concepts the package relies on. We formulate the quantum metrological problem as a quantum channel estimation, and introduce the QFI as the figure of merit to be optimized. Further on, we introduce both MOP and ISS optimization procedures. Finally, we briefly review the methods to compute fundamental bounds.

Sec. 3 is aimed to guide the reader through the high-level optimization functions, going step by step: explaining first how to provide the form of the parameter dependent channel, how to perform the simplest single-channel optimization problems, how to deal with the optimization of parallel and adaptive strategies and finally how to optimize metrological protocols in the most challenging scenarios where noise correlations between subsequent channel uses are present.

Sec. 4 complements the previous one, and shows the full potential of the package using the example of *collisional* metrological scenario, where one needs to design a customized protocol tensor-network structure from the basic building blocks, and use the low-level <code>iss_opt</code> optimization function.

We summarize the presentation in Sec. 5 indicating some limitations and further possible developments of the package.

2 Theoretical background

2.1 Quantum channel estimation problem

In a paradigmatic quantum metrological problem the goal is to estimate the value of a single parameter θ encoded in some physical process described by a quantum channel (formally a Completely Positive Trace Preserving map – CPTP):

$$\Lambda_{\theta}: \mathcal{L}\left(\mathcal{I}\right) \mapsto \mathcal{L}\left(\mathcal{O}\right),$$
 (1)

where \mathcal{I} , \mathcal{O} are Hilbert spaces of input and output quantum systems and $\mathcal{L}(\mathcal{H})$ is a set of linear operators on \mathcal{H} , that is a super-set of density matrices on \mathcal{H} .

The channel Λ_{θ} can be probed by an arbitrary θ -independent input state

$$\rho_0 \in \mathcal{L} \left(\mathcal{I} \otimes \mathcal{A} \right), \tag{2}$$

where \mathcal{A} is an auxiliary system called ancilla; Λ_{θ} does not act on \mathcal{A} , but the entanglement between \mathcal{I} and \mathcal{A} may be sometimes used to enhance the estimation precision in the presence of noise [22, 23, 30, 31]. The resulting output state is

$$\rho_{\theta} := (\Lambda_{\theta} \otimes \mathbb{I}_{\mathcal{A}}) (\rho_{0}) \in \mathcal{L} (\mathcal{O} \otimes \mathcal{A}), \qquad (3)$$

where $\mathbb{I}_{\mathcal{A}}$ represents the identity map on $\mathcal{L}(\mathcal{A})$ —note the notational distinction from $\mathbb{1}_{\mathcal{A}}$, which denotes identity operator on the \mathcal{A} space.

The state ρ_{θ} is measured by a generalized measurement $\Pi = \{\Pi_i\}$ resulting in the probability of

outcome i equal to $p_{\theta}(i) := \text{Tr}(\rho_{\theta}\Pi_i)$. The parameter θ is then estimated using an estimator $\tilde{\theta}(i)$ and the goal is to find the protocol giving results as close as possible to the true value of θ . In case of the simplest single-channel estimation strategy, as depicted in Fig. 1(A), the optimization of the protocol is equivalent to the optimization of the input state ρ_0 and the measurement $\{\Pi_i\}$. However, more complex protocols may additionally involve optimization over control operations C_i , as in e.g. scenarios (C) and (D) in Fig. 1.

In general, the exact form of the optimal protocol depends on the actual estimation framework chosen, be it frequentist or Bayesian [32–34], as well as the choice of the cost function/figure of merit to be minimized/maximized. In this work, we adopt the frequentist approach, and focus on optimization of the QFI as the figure of merit to be maximized.

2.2 Quantum Fisher Information

Given some probabilistic model that specifies probabilities $p_{\theta}(i)$ of obtaining different measurement outcomes i depending on the value of a parameter θ , one can lower bound the achievable mean squared error $\Delta^2 \tilde{\theta}$ of any locally unbiased estimator $\tilde{\theta}(i)$ via the famous classical Cramér-Rao (CCR) bound [35]:

$$\Delta^2 \tilde{\theta} \geqslant \frac{1}{k F_C(p_\theta)},$$
(4)

where k is the number of independent repetitions of an experiment and F_C is classical Fisher information (CFI):

$$F_C(p_\theta) := \sum_i \frac{\dot{p}_\theta(i)^2}{p_\theta(i)},\tag{5}$$

where \dot{p}_{θ} denotes the derivative with respect to θ . The bound is asymptotically saturable, in the limit of many repetitions of an experiment $k \to \infty$, with the help of e.g. maximum-likelihood estimator [35]. Hence, the larger the CFI the better parameter sensitivity of the model.

In quantum estimation models, the outcomes are the results of the measurement $\{\Pi_i\}$ performed on a quantum state ρ_{θ} , $p_{\theta}(i) = \text{Tr}(\rho_{\theta}\Pi_i)$. Hence, depending on the choice of the measurement, one may obtain larger or smaller CFI. The QFI corresponds to the maximal achievable

CFI, when optimized over all admissible quantum measurements [24–26]:

$$F_Q(\rho_\theta) := \max_{\{\Pi_i\}_i} F_C(p_\theta) = \text{Tr}\left(\rho_\theta L^2\right), \quad (6)$$

where L is the symmetric logarithmic derivative (SLD) of ρ_{θ} :

$$\dot{\rho}_{\theta} = \frac{1}{2} \left(\rho_{\theta} L + L \rho_{\theta} \right). \tag{7}$$

Moreover, the optimal measurement can in particular be chosen as the projective measurement in the eigenbasis of the SLD.

Combining the above with the CCR bound (4) leads to the quantum Cramér-Rao (QCR) bound, that sets a lower bound on achievable estimation variance when estimating parameter encoded in a quantum state ρ_{θ} :

$$\Delta^2 \tilde{\theta} \geqslant \frac{1}{kF_O(\rho_\theta)}.$$
 (8)

and is saturable in the limit of $k \to \infty$.

This makes the QFI a fundamental concept in the quantum estimation theory, and makes it meaningful to formulate optimization problems in quantum metrology in a form of optimization of the QFI of the final quantum state obtained at the output of a given metrological protocol.

The basic single-channel estimation task, depicted in Fig. 1(A), corresponds then to the following optimization problem

$$F_Q(\Lambda_\theta) = \max_{\rho_0} F_Q \left[\Lambda_\theta \otimes \mathbb{I}_{\mathcal{A}}(\rho_0) \right]. \tag{9}$$

We will refer to $F_Q(\Lambda_\theta)$ as the *channel* QFI, as it corresponds to the maximal achievable QFI of the output state of the channel, when the maximization over all input states is performed.

In case of protocols with multiple-channel uses, N>1, one could simply probe each channel independently, using independent probes and independent measurements. In this case, by additivity of QFI, one would end up with the corresponding N channels QFI — $F_Q^{(N)}(\Lambda_\theta)$ equal, for this simplistic strategy, to N times the single channel QFI.

However, one may also consider more sophisticated strategies involving multiple channel uses as depicted in Fig. 1(B),(C),(D), which may provide significant advantage over independent probing strategy, in principle leading to even

quadratic scaling of QFI — $F_Q^{(N)}(\Lambda_\theta) \propto N^2$, referred to as the *Heisenberg scaling* (HS) [1].

In case of noiseless unitary estimation models $\Lambda_{\theta}(\rho) = U_{\theta} \rho U_{\theta}^{\dagger}$ the optimal probe states that maximize the QFI are easy to identify analytically [1] and no sophisticated tools are required. In case of noisy models, however, the actual optimization over the protocol is much more involved, as in principle it requires optimization over multipartite entangled states (B) or multiple control operations C_i (C) or both (D).

This package allows for optimization of all kinds of metrological strategies, employing ancillary systems, entanglement and control operations, with the only physical restriction that the operations applied have a definite causal order, and hence can be regarded as a so-called *quantum combs* in the sense formalized in [36] and further in this text.

Regarding optimization strategies, we start with the discussion of MOP method, which is applicable to small-scale scenarios, and then move on to discuss a more versatile ISS optimization which can be combined with tensor-network formalism to deal with large-scale metrological problems.

2.3 Minimization over purifications

The MOP method [11, 12, 22, 37] is based on an observation that QFI of a state $\rho_{\theta} \in \mathcal{L}(\mathcal{H})$ is equal to minimization of QFIs over its purifications:

$$F_Q(\rho_\theta) = \min_{|\Psi_\theta\rangle} F_Q(|\Psi_\theta\rangle\langle\Psi_\theta|), \qquad (10)$$

where $|\Psi_{\theta}\rangle \in \mathcal{H} \otimes \mathcal{R}$ is a purification of ρ_{θ} , $\rho_{\theta} = \text{Tr}_{\mathcal{R}} |\Psi_{\theta}\rangle \langle \Psi_{\theta}|$.

Consider now a parameter encoding channel $\Lambda_{\theta}: \mathcal{L}(\mathcal{I}) \mapsto \mathcal{L}(\mathcal{O})$. The idea of minimization over purifications leads to an efficiently computable formula for the channel QFI [11, 12, 22, 37]

$$F_Q(\Lambda_{\theta}) = 4 \min_{\{K_{k,\theta}\}} \left\| \sum_{k=1}^r \dot{K}_{\theta,k}^{\dagger} \dot{K}_{\theta,k} \right\|, \tag{11}$$

where $\|\cdot\|$ is the operator norm and the minimization is performed over all equivalent Kraus representations of the channel, so that:

$$\Lambda_{\theta}(\cdot) = \sum_{k=1}^{r} K_{\theta,k} \cdot K_{\theta,k}^{\dagger}. \tag{12}$$

This optimization becomes feasible, as one can effectively parametrize derivatives of Kraus operators corresponding to all equivalent Kraus representations as:

$$\dot{K}_{\theta,k}(h) = \dot{K}_{\theta,k} - i \sum_{l} h_{kl} K_{\theta,l}, \qquad (13)$$

where $h \in \mathbb{C}^{r \times r}$ is a Hermitian matrix, while $K_{\theta,k}$ is any fixed Kraus representation of Λ_{θ} , e.g. the canonical representation obtained from eigenvectors of the corresponding Choi-Jamiołkowski (CJ) operator [38], see Appendix A for the definition of the CJ operator.

As a result, one may rephrase the apparently difficult minimization problem (11) as:

$$F_Q(\Lambda_\theta) = 4 \min_h \|\alpha(h)\|, \tag{14}$$

where

$$\alpha(h) = \sum_{k} \dot{K}_{\theta,k}(h)^{\dagger} \dot{K}_{\theta,k}(h). \tag{15}$$

Importantly, this problem may be effectively written as a simple semi-definite program (SDP) [12, 22]

$$F_Q(\Lambda_\theta) = 4 \min_{\substack{\lambda \in \mathbb{R}, \\ h - h^{\dagger}}} \lambda \quad \text{s.t.} \quad A \ge 0,$$
 (16)

where

$$A = \begin{pmatrix} \lambda \mathbb{1}_{\mathcal{I}} & \dot{K}_{\theta,1}^{\dagger}(h) & \dots & \dot{K}_{\theta,r}^{\dagger}(h) \\ \dot{K}_{\theta,1}(h) & & & \\ \vdots & & & & \\ \dot{K}_{\theta,r}(h) & & & & \end{pmatrix},$$

$$(17)$$

 $d=\dim\mathcal{O}$ and r is the number of Kraus operators. Provided the Hilbert space dimension is small enough, this problem may be solved efficiently using widely available SDP solvers, such as [39]. This optimization is implemented in the mop_channel_qfi function.

Notice, that the dimension of ancilla \mathcal{A} is not included in any of the constraints in (16). This is because MOP gives the maximal QFI without any restriction on ancilla sizes. Furthermore, in order to identify the optimal input state $|\psi\rangle$ one needs to solve an additional SDP problem, see [18, 22].

MOP can be also used to optimize QFI in case of multiple channel uses. For parallel strategy, Fig. 1(B), one can simply apply the single-channel method, replacing the channel Λ_{θ}

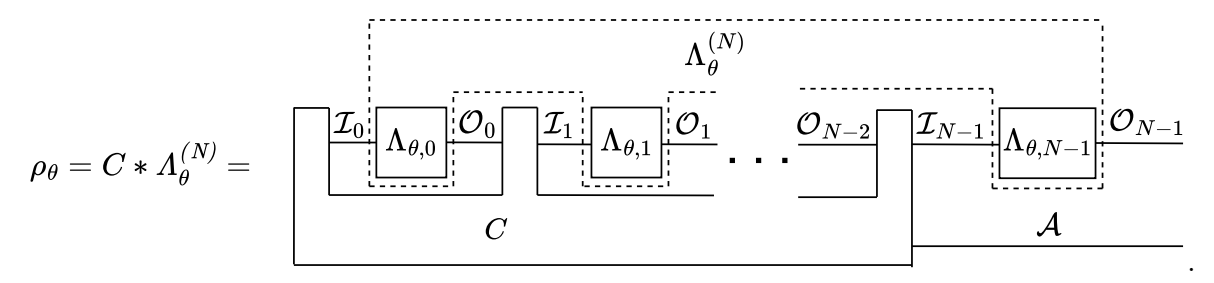


Figure 3: Final state resulting from the action of an adaptive protocol on N parameter encoding channels, written via a formal link product operation between the corresponding CJ operators—quantum combs.

with $\Lambda_{\theta}^{(N)} = \Lambda_{\theta}^{\otimes N}$ —this is implemented in the mop_parallel_qfi function.

In order to deal with an adaptive strategy, as in Fig. 1(C), one should first use the fact that a concatenated sequence of quantum channels C_i where the free inputs and free output spaces are respectively \mathcal{H}_{2i} , \mathcal{H}_{2i+1} , $i \in 0, ..., N-1$, can be represented as a quantum comb [36]

$$C \in \text{Comb}[(\mathcal{H}_0, \mathcal{H}_1), ..., (\mathcal{H}_{2N-2}, \mathcal{H}_{2N-1})], (18)$$

which is a CJ operator satisfying:

$$C \ge 0$$
, $C^{(N)} = C$, $C^{(0)} = 1$, (19)
 $\operatorname{Tr}_{2k-1}C^{(k)} = \mathbb{1}_{2k-2} \otimes C^{(k-1)}$, $k \in \{1, ..., N\}$.

The above conditions guarantee that such quantum comb C can always be regarded as a concatenation of quantum channels C_i , that is $C = C_0 * ... * C_{N-1}$, where * denotes the link product [36], see Appendix A for the definition of the link product.

In the context of metrological adaptive scenario, given a series of channels $\Lambda_{\theta,i}: \mathcal{L}(\mathcal{I}_i) \mapsto \mathcal{L}(\mathcal{O}_i)$, we can write the combined action of all the channels as:

$$\Lambda_{\theta}^{(N)} = \Lambda_{\theta,0} \otimes \dots \otimes \Lambda_{\theta,N-1}. \tag{20}$$

We may now represent the general adaptive strategy that includes the input state as well as the control operations in a form of a quantum comb

$$C \in \text{Comb}[(\varnothing, \mathcal{I}_0), (\mathcal{O}_0, \mathcal{I}_1), ..., (\mathcal{O}_{N-3}, \mathcal{I}_{N-2}), (\mathcal{O}_{N-2}, \mathcal{I}_{N-1} \otimes \mathcal{A})]$$
 (21)

and concatenate the operations using the link product in order to obtain the output state

$$\rho_{\theta} = C * \Lambda_{\theta}^{(N)} \in \mathcal{L}(\mathcal{O}_{N-1} \otimes \mathcal{A}), \qquad (22)$$

where $\Lambda_{\theta}^{(N)}$ (italics) formally represents the CJ operator of $\Lambda_{\theta}^{(N)}$, see Fig. 3. Here $\Lambda_{\theta}^{(N)}$ does not

necessarily need to represent the action of uncorrelated channels as in (20), but may also be a general parameter dependent quantum comb and in this way represent models with correlated noise or non-local character of estimated parameter.

Optimization over adaptive protocols is thus equivalent to maximization of the final QFI over quantum combs C. Using again the MOP idea, this problem may be effectively written down as an SDP (this time slightly more involved) of the following form [19, 20, 22]:

$$F_{\mathbf{Q}}^{(N)}(\Lambda_{\theta}) = 4 \min_{\substack{\lambda \in \mathbb{R}, \mathbf{Q}^{(k)} \\ h = h^{\dagger}}} \lambda \quad \text{s.t.} \quad A \ge 0, \tag{23}$$

$$\bigvee_{0 \le k \le N-1} \text{Tr}_{\mathcal{O}_{k-1}} Q^{(k)} = \mathbb{1}_{\mathcal{I}_{k-1}} \otimes Q^{(k-1)}, \ Q^{(0)} = 1,$$

where $Q^{(k)} \in \mathcal{L}(\mathcal{O}_0 \otimes \mathcal{I}_0 \otimes \cdots \otimes \mathcal{O}_{k-1} \otimes \mathcal{I}_{k-1})$ are optimization variables and A =

$$\begin{pmatrix} & \mathbb{1}_{\mathcal{I}_{N-1}} \otimes Q^{(N-1)} & |\dot{\tilde{K}}_{1,1}(h)\rangle \dots |\dot{\tilde{K}}_{r,d}(h)\rangle \\ & \langle \dot{\tilde{K}}_{1,1}(h)| & & & \\ & \vdots & & & \lambda \mathbb{1}_{dr} \\ & \langle \dot{\tilde{K}}_{r,d}(h)| & & & \end{pmatrix}$$
(24)

with

$$|\dot{\tilde{K}}_{i,k}(h)\rangle = \mathcal{O}_{N-1}\langle i|\dot{K}_{\theta,k}^{(N)}(h)\rangle,$$
 (25)

where

$$|\dot{K}_{i,k}^{(N)}(h)\rangle \in \mathcal{O}_0 \otimes \mathcal{I}_0 \otimes \cdots \otimes \mathcal{O}_{N-1} \otimes \mathcal{I}_{N-1},$$
 (26)

are derivatives of vectorized Kraus operators of $\Lambda_{\theta}^{(N)}$, r is the number of Kraus operators of $\Lambda_{\theta}^{(N)}$, $d = \dim \mathcal{O}_{N-1}$. This optimization is implemented in mop_adaptive_qfi function.

Similarly to the single channel case, optimization of parallel and adaptive strategies with MOP does not allow for the control of the ancilla dimension and finding optimal input state or optimal comb requires solving an additional SDP

problem [20, 22]. Moreover, since the algorithm requires optimization over Kraus representations of $\Lambda_{\theta}^{(N)}$ its time and memory complexity is exponentially large in N.

2.4 Iterative see-saw

In the ISS optimization method developed in the quantum metrology context in [17, 22, 40–44] one considers the *pre-QFI function*:

$$F(\rho_0, \mathfrak{L}) := 2 \operatorname{Tr} \left(\dot{\rho}_{\theta} \mathfrak{L} \right) - \operatorname{Tr} \left(\rho_{\theta} \mathfrak{L}^2 \right), \qquad (27)$$

where $\rho_{\theta} = \Lambda_{\theta} \otimes \mathbb{I}_{\mathcal{A}}(\rho_0)$, and where the dimension of \mathcal{A} can be chosen arbitrarily and this choice may affect the final result, unlike in the MOP method. It turns out that for a given ρ_0 the maximization of F over hermitian matrices \mathfrak{L} yields QFI of the state ρ_{θ} :

$$\max_{\mathfrak{L}=\mathfrak{L}^{\dagger}} F(\rho_0, \mathfrak{L}) = F_Q(\rho_{\theta}), \tag{28}$$

with the solution \mathfrak{L}^{\diamond} being equal to SLD matrix L of ρ_{θ} [41]—hence we will use the name pre-SLD matrix for \mathfrak{L} . It follows that the channel QFI (9) is simply a maximization of F over both of its arguments:

$$F_Q(\Lambda_\theta) = \max_{\rho_0, \mathfrak{L}} F(\rho_0, \mathfrak{L}). \tag{29}$$

This problem can be solved by initializing ρ_0 and $\mathfrak L$ at random and then by interchangeably making one argument constant and maximizing the other one. Each such optimization will increase the value of F and we can proceed until the change of F in a number of consecutive iterations becomes smaller then some established precision ϵ . In case of the single channel optimization the procedure is implemented in iss_channel_qfi.

ISS algorithm can be easily applied to parallel strategy by simply substituting Λ_{θ} with $\Lambda_{\theta}^{(N)} = \Lambda_{\theta}^{\otimes N}$ —this is implemented in iss_parallel_qfi function. This approach, however, suffers from the same problem as MOP—namely, it has an exponential complexity in N.

The solution is to split ρ_0 and \mathfrak{L} into smaller parts by expressing them as tensor networks (see Appendix B). Let us set $\mathcal{I}^{(N)} = \bigotimes_{i=0}^{N} \mathcal{I}_i$ and $\mathcal{O}^{(N)} = \bigotimes_{i=0}^{N} \mathcal{O}_i$, where for i < N spaces \mathcal{I}_i and \mathcal{O}_i are inputs and outputs of the *i*-th channel $\Lambda_{\theta,i}$ and $\mathcal{I}_N = \mathcal{O}_N = \mathcal{A}$. Then a state

$$|\psi\rangle = \sum_{a_0,\dots,a_N} \psi^{a_0\dots a_n} |a_0\dots a_N\rangle \in \mathcal{I}^{(N)}, \quad (30)$$

can be expressed as a tensor network called ma- $trix\ product\ state\ (MPS)\ [45, 46]:$

$$\psi^{a_0...a_N} = \underbrace{\psi_0}_{} \underbrace{\psi_1}_{} \underbrace{\psi_1}_{} \underbrace{\psi_1}_{} \underbrace{\psi_N}_{}, \qquad (31)$$

where indices a_i are called *physical* and horizontal indices that connect tensors ψ_i are called *bond*. Range of the bond indices called *bond* dimension and denoted by r_{MPS} controls the strength of possible correlations between sites of $|\psi\rangle$, $r_{\text{MPS}} = 1$ means that the state is separable and $r_{\text{MPS}} \approx \dim \mathcal{I}^{(N)}$ allows for arbitrary correlations. Analogously, pre-SLD matrix can be expressed as a matrix product operator (MPO):

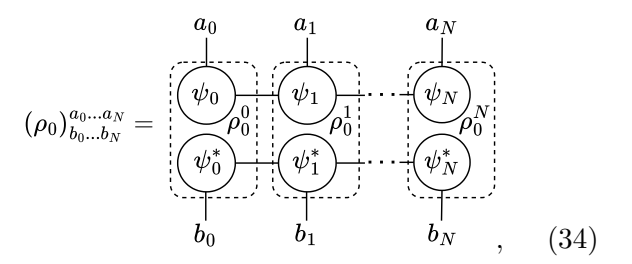
$$\mathfrak{L}_{b_0...b_N}^{a_0...a_N} = \underbrace{\begin{array}{c} a_0 & a_1 & a_N \\ \downarrow & \downarrow & \downarrow \\ b_0 & b_1 & b_N \end{array}}_{b_N} \dots \underbrace{\begin{array}{c} a_N \\ \downarrow \\ \downarrow \\ b_N \end{array}}_{(32)}$$

with bond dimension $r_{\mathfrak{L}}$. We can then write pre-QFI function as

$$F(\psi_0, ..., \psi_N, \mathfrak{L}_0, ..., \mathfrak{L}_N) = *_{i=0}^N \rho_0^i *$$

$$* \left[2\dot{\Lambda}_{\theta}^{(N)} * \left(*_{i=0}^N \mathfrak{L}_i \right)^T - \Lambda_{\theta}^{(N)} * \left(*_{i=0}^N \mathfrak{L}_i^2 \right)^T \right],$$
(33)

where ρ_0^i are elements of density matrix MPO of the state $|\psi\rangle$:



 ψ_i^* are entry-wise complex conjugations of ψ_i and \mathfrak{L}_i^2 are elements of MPO of \mathfrak{L}^2 . Additionally, we used linearity of link product and the identity $\text{Tr}(AB) = A*B^T$. Note that * denotes link product operation, but also contraction of corresponding spaces for more general tensor networks, e.g. MPSs, see Appendix B for more details.

Just like in the case of a single channel optimization, we can maximize the above function over one argument at a time while others stay constant. Then after optimization of each argument, we repeat the procedure until the value of F converges. Note that if $r_{\mathfrak{L}}$ is too small, then

the optimization over pre-SLD will not converge to the SLD matrix and value of pre-QFI will not be equal to QFI.

Nevertheless, the obtained value of F can be always interpreted as a CFI for a measurement given by eigenvectors of \mathfrak{L} [41]. This fact might be used to estimate the maximal value of CFI for local measurement, i.e. measurement in separable basis, because values of pre-QFI for $r_{\mathfrak{L}} = 1$ and $r_{\mathfrak{L}} = 2$ bound the maximal local measurements CFI from below and above respectively. Procedure employing MPS and MPO to the optimization of parallel strategy is implemented in iss_tnet_parallel_qfi.

For adaptive strategy we can apply the formula on ρ_{θ} from Fig. 3 to (27) and redefine pre-QFI function as

$$F(C, \mathfrak{L}) = 2C * \dot{\Lambda}_{\theta}^{(N)} * \mathfrak{L}^T - C * \Lambda_{\theta}^{(N)} * (\mathfrak{L}^2)^T.$$
 (35)

Then, the QFI for adaptive strategy becomes a maximization of (35) over hermitian \mathfrak{L} and quantum combs C (19)—this is implemented in iss_adaptive_qfi. Once more, this problem can be solved more efficiently if we split arguments of F into smaller parts. This time, however, tensor network of C has a natural interpretation as an input state ρ_0 and a series of control operations C_i like in Fig. 1(C). Thus we can optimize

$$F(\rho_0, C_0, ..., C_{N-2}, \mathfrak{L}) =$$

$$= \rho_0 * *_{i=0}^{N-2} C_i * \left[2\dot{\Lambda}_{\theta}^{(N)} * \mathfrak{L}^T - \Lambda_{\theta}^{(N)} * (\mathfrak{L}^2)^T \right].$$

We implemented this procedure in iss_adaptive_tnet_qfi.

Finally, ISS can be applied to any arrangement of input states, control operations and parametrized channels, see the example in Fig. 1(D). This is done by expressing ρ_{θ} as the contraction of tensors representing all channels, measurements (possibly represented by MPOs) and states (possibly represented by MPSs) and maximizing pre-QFI over each variable node separately. The package provides tools to define such arbitrary protocols which can be then optimized using iss_opt function. We discuss this in detail in Sec. 4.

Let us conclude this section with comparison of MOP and ISS. MOP is a deterministic algorithm with optimality of the numerical solution guaranteed by formal proofs. ISS initializes the parameters of pre-QFI function at random, thus it is nondeterministic. Additionally, there is no guarantee that it converges to the true optimum of the pre-QFI function. The optimality can be validated in some cases by comparing its result with MOP or upper bounds, see Sec. 2.5. It might be also useful to repeat the computation several times and check whether the returned values vary.

On a positive side, what is guaranteed in ISS is that the figure of merit will never decrease in every individual iteration step and that the final result will always be a correct *lower bound* of a truly optimal QFI.

Moreover, ISS is much more efficient than MOP. Its exact time complexity depends on the strategy and it is hard to estimate. Our numerical data shows that for strategies that are similar to parallel or adaptive strategy and with the use of tensor networks the time complexity is quadratic in N. This is significantly better than exponential complexity of MOP and allows to compute QFI for much bigger values of N ($N \leq 5$ for MOP vs $N \leq 100$ for ISS). Moreover, in ISS we can control additional parameters like ancilla or bond dimension and consider strategies different from parallel and adaptive. Finally, while both methods can be used to get the optimal adaptive or parallel protocols, it is much more straightforward for ISS, as it requires only inspecting the final values of the pre-QFI function optimized arguments.

2.5 Upper bounds

In Sec. 2.3 we explained that the QFI can be computed through minimization of the norm of α (15) over all Kraus representations $\{K_{\theta,k}\}$ of the channel Λ_{θ} . It follows that in order to compute QFI for parallel or adaptive strategy we need to optimize over Kraus representations $\{K_{\theta,k}^{(N)}\}$ of the whole channel $\Lambda_{\theta}^{(N)} = \Lambda_{\theta}^{\otimes N}$ which is exponentially hard in N. However, if we only want to obtain the upper-bounds, we may dramatically reduce the complexity of the optimization, and reformulate computation of the bound in a way that only minimization over Kraus representation of the single channel Λ_{θ} is required [12, 13, 21, 28, 31].

In case of parallel strategies this leads to an

upper-bound of the form [11, 12, 31]:

$$F_Q^{(N)}(\Lambda_\theta) \le 4N \min_h (\|\alpha(h)\| + (N-1)\|\beta(h)\|^2),$$
(36)

where $\alpha(h)$ is defined in (15), while

$$\beta(h) = \sum_{k} \dot{K}_{\theta,k}^{\dagger}(h) K_{\theta,k}(h). \tag{37}$$

This bound allows to immediately exclude the possibility of the Heisenberg scaling in the model—it is enough to show that there exist h for which $\beta(h) = 0$, which may be formulated as a simple algebraic condition [12, 18].

In case of adaptive strategy, one may again employ the idea of MOP to bound the maximal increase of QFI when the adaptive strategy is extended by one additional step including one more sensing channel [21]:

$$F_{\mathbf{Q}}^{(N+1)}(\Lambda_{\theta}) \leq F_{\mathbf{Q}}^{(N)}(\Lambda_{\theta}) + 4 \min_{h} \left[\|\alpha(h)\| + \sqrt{F_{\mathbf{Q}}^{(N)}(\Lambda_{\theta})} \|\beta(h)\| \right]. \quad (38)$$

Both of these bounds can be computed efficiently irrespectively of the value of N [21]. They are implemented in par_bounds and ad_bounds functions respectively.

Importantly, the bounds for parallel and adaptive strategy are asymptotically (for $N \to \infty$) equivalent and saturable [18, 21]—there are strategies which asymptotically achieve the optimal value of QFI predicted by the bounds.

Depending on whether there exist h for which $\beta(h) = 0$ we may have two possible asymptotic behaviors, namely the *standard scaling* (SS):

$$\lim_{N \to \infty} F_Q^{(N)}(\Lambda_{\theta})/N = 4 \min_{h, \beta(h) = 0} \|\alpha(h)\|, \quad (39)$$

and the *Heisenberg scaling* (HS):

$$\lim_{N \to \infty} F_Q^{(N)}(\Lambda_\theta) / N^2 = 4 \min_h \|\beta(h)\|^2.$$
 (40)

In the package, asymptotic bound can be computed using asym_scaling_qfi, a function that automatically determines also the character of the scaling.

Finally, there are methods to compute the bounds also in the case of correlated noise models that have been developed recently in [28]. We do not provide exact formulation of the optimization problem that one needs to solve to

find the relevant bound as it is much more involved than in case of uncorrelated noise models discussed above. In the package, the correlated noise bounds may be computed using ad_bounds_correlated in the regime of finite channel uses, and ad_asym_bounds_correlated in order to obtain the asymptotic behavior. Unlike in the uncorrelated noise models, there is no guarantee here that the bounds are saturable. Still, they may be systematically tightened at the expense of increasing the numerical complexity, see Sec. 3.5 for more discussion.

3 Basic package usage—optimization of standard strategies

In this section we present the basic ways to use the package, that utilize high-level functions from protocols and bounds sub-packages. These functions allow the user to compute and bound the QFI within three standard scenarios: single channel use, parallel and adaptive, by simply specifying the parameter encoding channel and the number of uses.

In the following subsections we will apply these methods to study the problem of phase estimation in presence of two paradigmatic decoherence models: dephasing (d) or amplitude damping (a).

The parameter encoding channels Λ_{θ} that we will consider involve is given by Kraus operators of the form

$$K_{\theta,k} = U_{\theta}K_k, \quad U_{\theta} = e^{-\frac{\mathrm{i}}{2}\theta\sigma_z},$$
 (41)

where σ_z is a Pauli z-matrix, U_{θ} represents unitary parameter encoding, whereas K_k are Kraus operators corresponding to one of the two decoherence models. For simplicity, we will always assume that estimation is performed around parameter value $\theta \approx 0$, so after taking the derivatives of Kraus operators we set $\theta = 0$ —this does not affect the values of the QFI as finite unitary rotation could always be incorporated in control operations, measurements or state preparation stage and hence will not affect the optimized value of QFI.

In case of the dephasing model, the two Kraus operators may be parametrized with a single parameter $p \in [0, 1]$:

$$K_0^{(d)} = \sqrt{p}\mathbb{1}, \quad K_1^{(d)} = \sqrt{1 - p}\sigma_z,$$
 (42)

where p=1 corresponds to no dephasing, p=1/2 to the the strongest dephasing case, where all equatorial qubit states are mapped to the maximally mixed states, while p=0 represents a phase flip channel. Equivalently, we may use a different Kraus representation where the two Kraus operators are given by:

$$K_{+}^{(d)} = \frac{1}{\sqrt{2}}U_{\epsilon}, \quad K_{-}^{(d)} = \frac{1}{\sqrt{2}}U_{-\epsilon},$$
 (43)

which may be interpreted as random rotations by angles $\pm \epsilon$ with probability 1/2—in order for the two representations to match we need to fix $p = \cos^2(\epsilon/2)$.

In case of *amplitude* damping, the Kraus operators take the form

$$K_0^{(a)} = |0\rangle\langle 0| + \sqrt{p} |1\rangle\langle 1|, K_1^{(a)} = \sqrt{1-p} |0\rangle\langle 1|,$$
(44)

where p=1 represents no decoherence case, while p=0 full relaxation case, where all the states of the qubit are mapped to the ground $|0\rangle$ state.

Alternatively, dephasing and amplitude damping models can be considered in a continuous time regime. In this case, the state undergoes a process for some time t which imprints on it an information about the parameter ω related with θ by $\theta = \omega t$. The derivative of the state over the time is defined using the *Lindbladian operator* \mathcal{L}_{ω} :

$$\frac{d\rho_{\omega,t}}{dt} = \mathcal{L}_{\omega}[\rho_{\omega,t}] = \frac{1}{i\hbar}[H_{\omega}, \rho_{\omega,t}] + \mathcal{D}[\rho_{\omega,t}], \quad (45)$$

where $H_{\omega} = \hbar \omega \sigma_z/2$ is a Hamiltonian generating the evolution U_{θ} and \mathcal{D} is a dissipation term. The form of the dissipation term depends on the noise model:

$$\mathcal{D}^{(d)}[\rho] = \frac{\gamma^{(d)}}{2} (\sigma_z \rho \sigma_z - \rho), \tag{46}$$

$$\mathcal{D}^{(a)}[\rho] = \frac{\gamma^{(a)}}{2} \left(\sigma_{-} \rho \sigma_{-}^{\dagger} - \frac{1}{2} \{ \sigma_{-}^{\dagger} \sigma_{-}, \rho \} \right), \quad (47)$$

where $\sigma_{-} = |0\rangle\langle 1|$ and $\{\cdot,\cdot\}$ is the anticommutator. In both cases the factor γ determines the strength of the decoherence and is related to the original noise strength p by relations:

$$2p - 1 = e^{-\gamma^{(d)}t}, \quad p = e^{-\gamma^{(a)}t}.$$
 (48)

3.1 Specifying the parameter dependent channel

First, let us start by explaining how to encode the channel using the ParamChannel class. We can do that in one of the four available ways:

- from list of Kraus operators and their derivatives over θ ,
- from CJ matrix and its derivative over θ ,
- using a predefined creator function,
- from a time-independent Lindbladian, its derivative over ω and specified evolution time

The following listing shows how the above options are implemented in practice using the example of the dephasing channel (42):

```
import numpy as np
  from qmetro import *
4 # Pauli z-matrix:
  sz = np.array([[1, 0], [0, -1]])
  # Kraus operators and their derivatives
  # for dephasing channel:
  p = 0.75
  krauses = [
      sqrt(p) * np.identity(2),
      sqrt(1-p) * sz
13
  dkrauses = [
      -1j/2 * sz @ K for K in krauses
  # ParamChannel instance created from
19 # Kraus operators:
  channel1 = ParamChannel(
      krauses=krauses, dkrauses=dkrauses
24 # CJ matrix and its derivative created
25 # from Kraus operators:
26 choi = choi_from_krauses(krauses)
27 dchoi = dchoi_from_krauses(
      krauses, dkrauses
31 # ParamChannel instance created from
32 # CJ matrix:
33 channel2 = ParamChannel(
      choi=choi, dchoi=dchoi
37 # ParamChannel instance created using
38 # creator function:
39 channel3 = par_dephasing(p)
```

```
41 # Lindbladian and its derivative.
42 omega = 0.0 # Parameter.
43 t = 1 # Time.
44 # Dephasing strength:
45 \text{ gamma} = -\text{np.log}(2*\text{p-1})/\text{t}
46 def lindblad(rho):
       # Rotation around z part:
47
       rot = 0.5j*omega * (rho@sz - sz@rho)
48
       # Dephasing part:
49
       deph = gamma * (sz@rho@sz - rho)
50
51
       return rot + deph
52
53 def dlindblad(rho):
       return 0.5j * (rho@sz - sz@rho)
54
55
56 # ParamChannel instance created from
57 # Lindbladian:
58 channel4 = ParamChannel(
       lindblad=lindblad,
59
       dlinblad=dlindblad,
60
       time=t, input_dim=2
61
62 )
  Objects of ParamChannel class can be used to
  compute \rho_{\theta} = \Lambda_{\theta}(\rho) and \dot{\rho}_{\theta} = \frac{d}{d\theta}\Lambda_{\theta}(\rho), e.g.:
1 channel = channel1
2 rho = np.array([
       [1, 0],
4
       [0, 0]
5])
7 rho_t, drho_t = channel(rho)
  or to obtain CJ operator from Kraus operators
  and vice versa, e.g.:
channel1 = ParamChannel(
       krauses=krauses, dkrauses=dkrauses
2
3 )
4 # CJ matrix:
5 choi = channel.choi()
6 # Derivative of CJ matrix:
7 dchoi = channel.dchoi()
9 channel2 = ParamChannel(
       choi=choi, dchoi=dchoi
10
11 )
12 # Kraus operators:
13 krauses = channel2.krauses()
14 # Kraus operators and their derivatives:
15 krauses, dkrauses = channel2.dkrauses()
  They can be combined with each other to create
```

new channels using:

```
• scalar multiplication (\alpha \Lambda_{\theta})(\rho) = \alpha \Lambda_{\theta}(\rho),
  e.g.:
1 a = 0.2
2 new_channel = channel.scalar_mul(a)
3 # or equivalently
4 new_channel = a * channel
```

```
• addition (\Lambda_{\theta} + \Phi_{\theta})(\rho) = \Lambda_{\theta}(\rho) + \Phi_{\theta}(\rho), e.g.: 9 mop_qfi = mop_channel_qfi(channel)
```

```
1 new_channel = channel1.add(channel2)
2 # or equivalently
3 new_channel = channel1 + channel2
• composition (\Lambda_{\theta} \circ \Phi_{\theta})(\rho) = \Lambda_{\theta} (\Phi_{\theta}(\rho)), e.g.:
1 new_channel = channel1.compose(
          channel2
3)
4 # or equivalently
5 new_channel = channel1 @ channel2
• Kronecker product (\Lambda_{\theta} \otimes \Phi_{\theta}) (\rho_1 \otimes \rho_2) =
   \Lambda_{\theta}(\rho_1) \otimes \Phi_{\theta}(\rho_2), e.g.:
1 new_channel = channel1.kron(channel2)
• Kronecker power \Lambda_{\theta}^{\otimes N} = \underbrace{\Lambda_{\theta} \otimes ... \otimes \Lambda_{\theta}}_{N}, e.g.:
1 N = 3
2 new_channel = channel1.kron_pow(N)
```

Single channel QFI optimization

Having defined the parameter dependent channel using the ParamChannel class, we may now easily compute the single-channel QFI (9), taking into account that we may also make use of the ancilla, see Fig. 4(A). The channel QFI can be computed using one of the two functions:

- iss_channel_qfi for ISS method,
- mop_channel_qfi for MOP method.

Function iss_channel_qfi takes two arguments: channel to compute the QFI for and the dimension of the ancillary system. It returns five items: optimized QFI, list of pre-QFI values per algorithm iteration, density matrix of the optimal input state, SLD matrix and the information whether the optimization converged successfully.

On the other hand, mop_channel_qfi takes only the channel and returns only the QFI—here, by the nature of the method, ancillary system dimension is unspecified, see Sec. 2.3. The following code shows both of these functions in prac-

```
1 from qmetro import *
3 p = 0.75
4 channel = par_dephasing(p)
6 ancilla_dim = 2
7 iss_qfi, qfis, rho0, sld, status =
     iss_channel_qfi(channel, aniclla_dim)
```

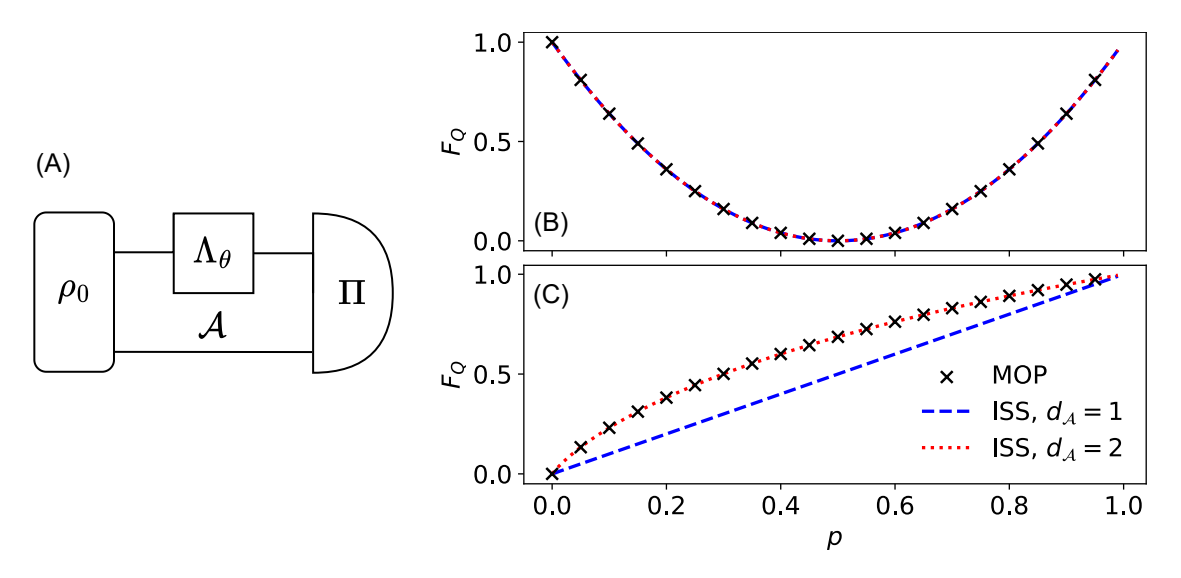


Figure 4: (A) Diagram of strategy with single parametrized channel Λ_{θ} and ancilla \mathcal{A} . Values of QFI for (B) dephasing (C) amplitude damping, various values of p and different methods: MOP - black \times , ISS with $d_{\mathcal{A}}=1$ - blue dashed line, ISS with $d_{\mathcal{A}}=2$ - red dotted line.

Fig. 4(B) and Fig. 4(C) present plots of the results obtained using <code>iss_channel_qfi</code> and <code>mop_channel_qfi</code> for the two decoherence models respectively. Since MOP method gives the optimal QFI implicitly assuming arbitrary ancilla dimension $d_{\mathcal{A}}$, these plots indicate that for the dephasing case (B) ancilla is in fact unnecessary, while in the amplitude damping case (C) ancillary system of dimension $d_{\mathcal{A}} = 2$ is required for an optimal precision.

This example clearly shows the benefits of having two independent optimization procedures. One method (MOP) provides the true optimal QFI, but does not allow us to get an insight into the required ancilla size, while the other one (ISS) allows us to study the impact of the ancilla size.

3.3 Parallel strategy optimization

Parallel strategy is a strategy where N copies of Λ_{θ} are probed in parallel by an entangled state and their output is collectively measured, see Fig. 5(A). It can be also understood as a strategy with a single channel $\Lambda_{\theta}^{(N)} = \Lambda_{\theta}^{\otimes N}$. QMetro++ package provides several functions computing QFI for parallel strategy. The simplest two, iss_parallel_qfi and mop_parallel_qfi are straightforward generalizations of ISS and MOP methods for parallel strategy:

```
1 from qmetro import *
2
3 p = 0.75
4 channel = par_dephasing(p)
```

```
6 N = 3
7 ancilla_dim = 2
8 iss_qfi, qfis, rho0, sld =
    iss_parallel_qfi(channel, N,
    aniclla_dim)
9
10 mop_qfi = mop_parallel_qfi(channel, N)
```

The downside of these two approaches is that they try to optimize QFI over all possible states and measurements on an exponentially large Hilbert space. Hence, their time and memory complexity are exponential in the number of channel uses. In practice, this means that they can be used for relatively small N ($N \lesssim 5$ in case of qubit channels).

This problem can be circumvented using tensor networks MPS (31) and MPO (32). This approach is implemented in <code>iss_tnet_parallel_qfi</code>, which requires two additional arguments specifying the size of MPS and pre-SLD MPO bond dimensions:

```
1 from qmetro import *
2
3 p = 0.75
4 channel = par_dephasing(p)
5
6 N = 3
7 ancilla_dim = 2
8 mps_bond_dim = 2
9 L_bond_dim = 4
10
11 qfi, qfis, psis, Ls, status =
    iss_tnet_parallel_qfi(channel, N, aniclla_dim, mps_bond_dim, L_bond_dim
```

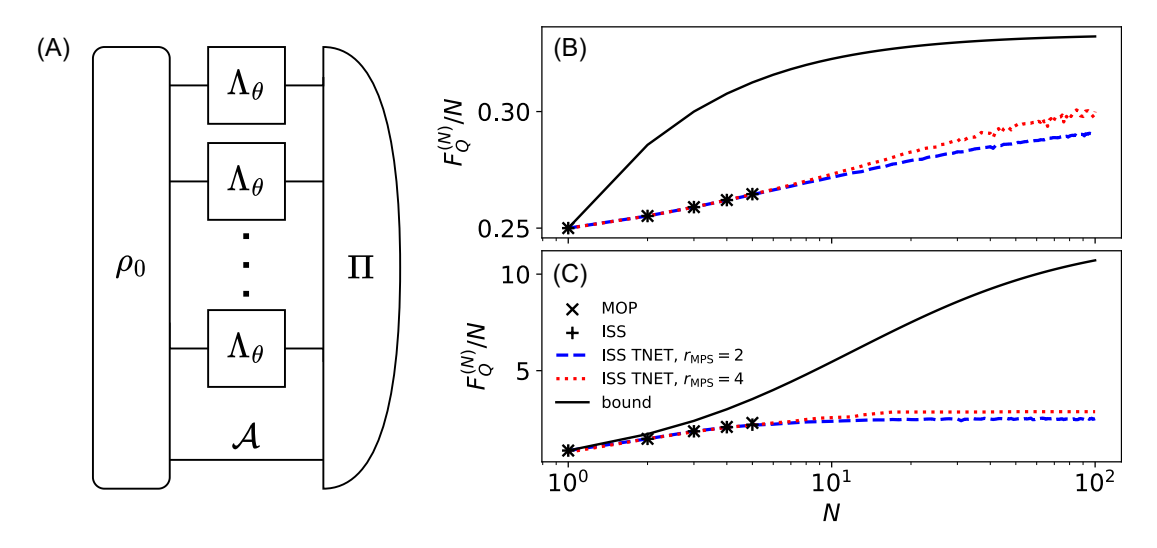


Figure 5: (A) Diagram of parallel strategy with multiple parametrized channels Λ_{θ} and ancilla \mathcal{A} . Values of QFI normalized by number of channel uses - N for: (B) dephasing (p=0.75) (C) amplitude damping (p=0.75) and different methods: MOP - black \times , simple ISS with $d_{\mathcal{A}}=2$ - black +, tensor network ISS with $d_{\mathcal{A}}=2$, $r_{\mathrm{MPS}}=\sqrt{r_{\mathfrak{L}}}=4$ - red dotted line, upper bound - black solid line.

)

In contrast to the function implementing the basic ISS, which returns the optimal input state and the SLD in terms of arrays, this procedure gives them in a form of lists containing tensor components: $psis = [\psi_0, \psi_1, ...]$ and $Ls = [\mathfrak{L}_0, \mathfrak{L}_1, ...]$, see Eqs. (31) and (32).

Naturally, increasing ancilla and bond dimensions allows to achieve higher values of QFI up to some optimal value, see Fig. 5(B) and (C). One might asses this value by running iss_tnet_parallel_qfi for increasing dimension sizes, but it can be also upper-bounded using the par_bounds function which gives a bound on the QFI of parallel strategy for all ancilla and bond dimension sizes (see section 2.5):

```
1 from qmetro import *
2
3 p = 0.75
4 channel = par_dephasing(p)
5
6 N = 3
7
8 bound = par_bounds(channel, N)
```

The obtained value is an array bound= $[b_1, b_2, ..., b_N]$ where b_n is an upper bound on $F_Q^{(n)}(\Lambda_\theta)$.

The numerical results are presented in Fig. 5(B) and (C). We considered parallel strategy with ancilla dimension d_A and various bond dimensions $r_{\text{MPS}} = \sqrt{r_{\Sigma}}$. Notice that for dephas-

ing case (B) results from MOP and ISS methods coincide perfectly and that QFI for MPS with $r_{\text{MPS}}=4$ approaches the upper bound with growing N. This suggests that in this case $d_{\mathcal{A}}=2$ is sufficient to saturate the bound. On the other hand, for the amplitude damping case (C) the results obtained using MOP and ISS differ, and already for N=5 the ancilla dimension $d_{\mathcal{A}}=2$ is suboptimal. Additionally, $F_Q^{(N)}(\Lambda_\theta)/N$ computed using MPS quickly flattens out and the increase of bond dimension leads to a very small improvement. Therefore, we can conclude that in this case the $d_{\mathcal{A}}$ considered are insufficient to saturate the bound.

3.4 Adaptive strategy optimization

In the adaptive strategy we start with an initial state of the system and the ancilla, ρ_0 , and we act on the system with N parameter encoding channels Λ_{θ} , intertwined with control operations C_i which act both on the system and the ancilla, see Fig. 6(A). Equivalently, it is a strategy where N parameter encoding channels Λ_{θ} are plugged in between the teeth of a quantum comb C, see Fig. 3, and then the resulting state is measured. In this strategy, one tries to obtain the value of QFI for the optimal input state, measurement and control operations (or equivalently the optimal comb and measurement). Notice that for large enough ancilla dimension d_A and for C_i be-

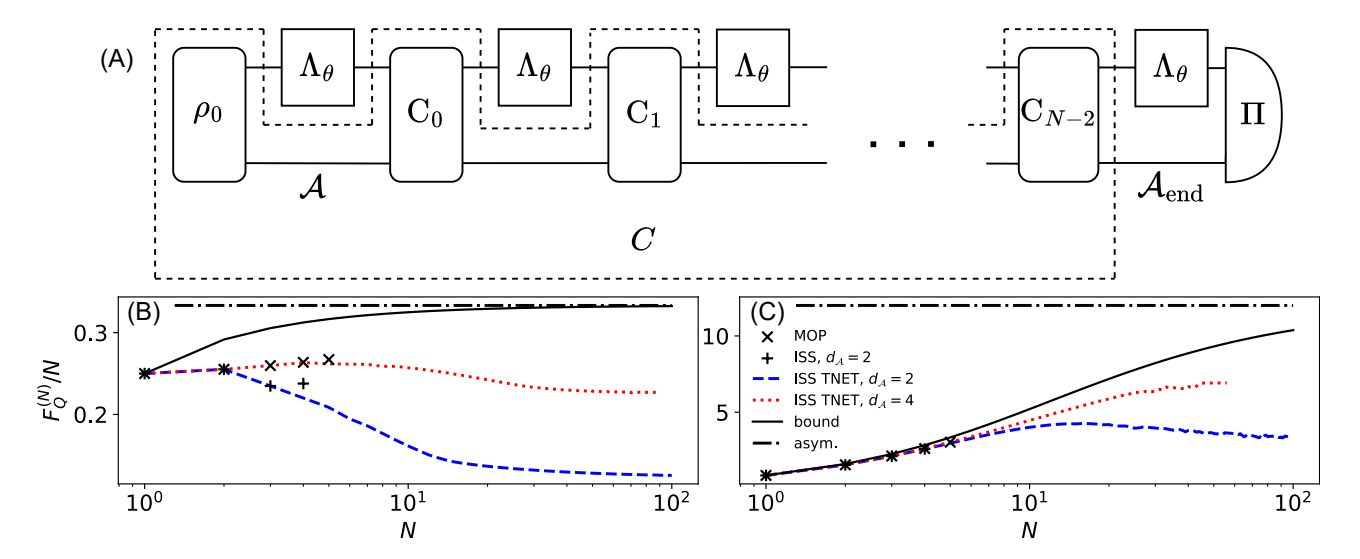


Figure 6: (A) Diagram of adaptive strategy with multiple parametrized channels Λ_{θ} and ancilla \mathcal{A} . When the optimization is performed over all quantum combs C (area bounded by dashed lines) one can control the dimension of only the final ancilla ($\mathcal{A}_{\mathrm{end}}$). Values of QFI normalized by number of channel uses - N for: (B) dephasing (p=0.75) (C) amplitude damping (p=0.75) and different methods: MOP - black \times , simple ISS with $d_{\mathcal{A}}=2$ - black +, tensor network ISS with $d_{\mathcal{A}}=2$ - blue dashed line, tensor network ISS with $d_{\mathcal{A}}=2$ - red dotted line, upper bound - black solid line, asymptotic bound - black dash-dotted line.

ing appropriate SWAP gates one can simulate any parallel strategy with an adaptive strategy. Thus for d_A large enough QFI for adaptive strategy always upper-bounds QFI for parallel strategy.

QFI for adaptive strategy using the MOP method can be computed by simply invoking mop_adaptive_qfi:

```
1 from qmetro import *
2
3 p = 0.75
4 channel = par_dephasing(p)
5
6 N = 3
7
8 qfi = mop_adaptive_qfi(channel, N)
```

This yields truly optimal QFI corresponding to the optimal adaptive strategy.

Alternatively, we may also use the ISS method, with the help of <code>iss_adaptive_qfi</code> function. This procedure will perform the optimization over the whole comb as well. Note that, constraints on a quantum comb (19) allow for its decomposition into control operations (CPTP maps), but do not specify the ancilla dimension inside the comb. Therefore, in this case one can control only the dimension of the last ancilla which goes outside of the comb, indicated by the symbol \mathcal{A}_{end} in Fig. 6(A):

```
1 from qmetro import *
```

```
3 p = 0.75
4 channel = par_dephasing(p)
5
6 N = 3
7 # Dimension of the last ancilla:
8 aniclla_dim = 2
9
10 qfi, qfis, comb, sld, status =
    iss_adaptive_qfi(channel, N,
    aniclla_dim)
```

Apart from the standard outputs for the ISS-type functions, iss_adaptive_qfi returns comb which is a CJ matrix of the optimal comb.

Finally, if we want to make use of the tensor-network structure, and perform the optimization over separate control operations, we can use <code>iss_tnet_adaptive_qfi</code>. Notice that in this approach we control ancilla dimension at each step and thus, in general, the obtained QFI will be smaller then the one we got with <code>iss_adaptive_qfi</code>—the advantage here is that the optimization will be much more efficient (not to mention that this is also the only way to go to the larger N limit):

```
1 from qmetro import *
2
3 p = 0.75
4 channel = par_dephasing(p)
5
6 N = 3
7 # Dimension of the ancilla:
```

```
8 aniclla_dim = 2
9
10 qfi, qfis, teeth, sld, status =
    iss_adaptive_qfi(channel, N,
    aniclla_dim)
11 # teeth can be decomposed into rho0 and
12 # a list of controls:
13 rho0, *Cs = teeth
```

The returned argument teeth represents the comb's teeth and it is a list consisting of the optimal initial state and CJ matrices of the optimal control operations teeth = $[\rho_0, C_0, C_1, ..., C_{N-2}]$.

Upper bound for the adaptive strategy is computed using ad_bounds function:

```
1 from qmetro import *
2
3 p = 0.75
4 channel = par_dephasing(p)
5
6 N = 3
7 bound = ad_bounds(channel, N)
```

Additionally, one can compute the value of the bound in the limit $N \to \infty$ which is asymptotically saturable and the same for both parallel and adaptive strategy, see Sec. 2.5:

```
from qmetro import *

property pro
```

where the returned values should be interpreted in the following way $c = \lim_{N \to \infty} F_Q^{(N)}(\Lambda_\theta)/N^k$.

Values of QFI, bounds and asymptotic QFI for adaptive strategy are presented in Figs. 6 (B) and (C). In contrast to the parallel strategy, this time the amplitude damping case (C) shows results which are much closer to the bound.

Notice that there is no data for amplitude damping and ancilla dim $d_{\mathcal{A}} = 4$ and $N \geq 60$. This is due to the fact that for this noise model, the QFI attains a large value and simultaneously optimal control operations C_i take the state close to the pure state. These two processes combined create objects (tensors, matrices etc.) which hold values from a very wide range at the same time what causes loss of precision and then numerical instability.

3.5 Correlated noise models

QMetro++ gives also a simple way to compute QFI for adaptive and parallel strategy in scenar-

ios when parameter encoding channels act on an additional environment space \mathcal{E} which directly connects subsequent channels, see Fig. 7(A). This approach allows in particular to model noise correlations affecting the sensing channels.

To illustrate this, let us consider a Kraus representation for the dephasing model with Kraus operators K_{\pm} acting as Bloch sphere rotations by $\pm \epsilon$ around z axis, see Eq. (43). We want the signs of these rotations to form a binary Markovian chain. The conditional probability of a rotation with sign $s_i \in \{+, -\}$ in channel i assuming s_{i-1} in channel i-1 is:

$$T_{i|i-1}(s_i|s_{i-1}) = \frac{1}{2}(1 + s_i s_{i-1}c),$$
 (49)

where $c \in [-1, 1]$ is a correlation parameter with c = 0 meaning no correlations, c = 1 maximal positive correlations and c = -1 maximal negative correlations. The initial probabilities are $p(\pm) = 1/2$.

This process can be modeled with the help of a two dimensional environment Hilbert space \mathcal{E} which will carry the information about the sign of the rotation in the preceding step. Let us introduce a new channel acting on both the environment and the system $\tilde{\Lambda}_{\theta} = \Phi_{\theta} * T$, see Fig. 8, where:

$$\Phi_{\theta} : \mathcal{L}(\mathcal{E} \otimes \mathcal{S}) \ni \rho \mapsto V_{\theta} \rho V_{\theta}^{\dagger} \in \mathcal{L}(\mathcal{E} \otimes \mathcal{S}),$$

$$V_{\theta} = \sqrt{2} \sum_{s=\pm} |s\rangle \langle s| \otimes K_{s,\theta}, \quad (50)$$

and

$$T: \mathcal{L}(\mathcal{E}) \ni \rho_E \mapsto \sum_{s,r=\pm} T_{sr} \rho_E T_{sr}^{\dagger} \in \mathcal{L}(\mathcal{E}),$$

$$T_{sr} = \sqrt{\frac{1 + src}{2}} |s\rangle \langle r|. \quad (51)$$

Clearly, $\tilde{\Lambda}_{\theta}$ acts as Λ_{θ} on the system— $\mathrm{Tr}_{\mathcal{E}}\tilde{\Lambda}_{\theta}(\rho) = \Lambda_{\theta}(\mathrm{Tr}_{\mathcal{E}}\rho)$ for any state ρ . Unitary channel Φ_{θ} acts with K_{\pm} on the system, depending on the state of the environment being $|\pm\rangle$, and it stores the information about the occurrence of K_{\pm} in the state $|\pm\rangle$ accordingly. Then T modifies the state of \mathcal{E} according to probabilities (49). The initial probabilities are encoded in the initial environment state $\rho_E = p(+)|+\rangle\langle+|+p(-)|-\rangle\langle-|=\mathbb{1}_2/2$.

Channel Λ_{θ} can be easily constructed using the link_env method which links two channels through their common environment:

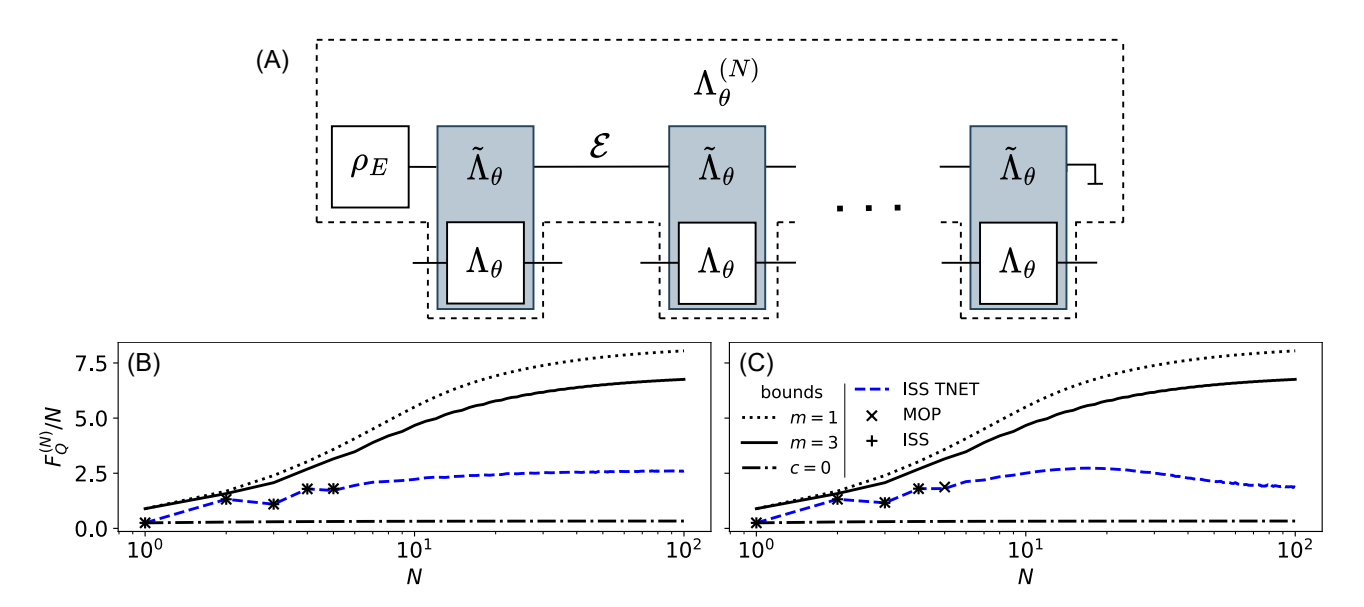


Figure 7: (A) Diagram of N parametrized channels Λ_{θ} with noise correlations. Extended channels $\tilde{\Lambda}_{\theta}$ (gray) act on the system as Λ_{θ} and they are connected with each other by the environment space \mathcal{E} . The environment system \mathcal{E} starts in the state ρ_E and it is not accessed (it is traced out) at the end. Values of QFI normalized by number of channel uses - N for anti-correlated (c=-0.75) dephasing (p=0.75), different strategies (B) parallel (C) adaptive and various methods: MOP - black \times , simple ISS with $d_{\mathcal{A}}=2$ - black +, tensor network ISS with $d_{\mathcal{A}}=2$ (parallel: $r_{\mathrm{MPS}}=\sqrt{r_{\mathfrak{L}}}=2$) - blue dashed line, upper bound with block size m=1 - black dotted line, upper bound with block size m=3 - black solid line and upper bound for uncorrelated channels c=0 - black dash-dotted line. Notice that since there are no separate bounds for parallel strategy with correlated channels the upper bounds (black dotted and solid lines) are identical in (B) and (C).

= kron(ket_bra(plus, plus), Kp)

26 # Derivative of V_theta matrix:

27 dV = kron(ket_bra(plus, plus), dKp)

28 dV += kron(ket_bra(minus, minus), dKm)

V = sqrt(2) * V

dV = sqrt(2) * dV

V = V + kron(ket_bra(minus, minus), Km)

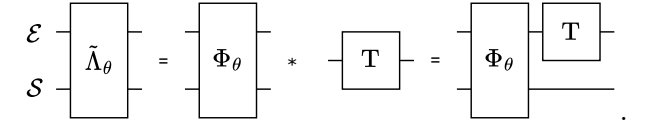


Figure 8: Modeling of correlated dephasing process, by extending the action of the channel on a two-dimensional environment space.

```
env_dim=d tells ParamChannel
                                                   constructor that the channel acts
1 from numpy import array, kron, sqrt
                                                  # on the d-dimensional environment space
                                               ^{34} # and the system
  from qmetro import *
                                               35 Phi = ParamChannel(
                                                      krauses=[V], dkrauses=[dV],
    = 0.75
                                               36
  p
                                                      env_dim=2
5
                                               37
                                               38
  # rot_like=True gives dephasing in
                                               39
                                               40 # T channel:
  # the second form:
9 Lambda = par_dephasing(p, rot_like=True)
                                                  T_{krauses} = []
  krauses, dkrauses = Lambda.dkrauses()
                                                  for s in (1, -1):
                                                      for r in (1, -1):
11 # Rotations by plus and minus epsilon:
                                               43
                                                          x = sqrt((1+s*r*c)/2)
12 Kp, Km = krauses
                                               44
13 # Derivatives of Krauses by theta:
                                                          Tsr = x * ket_bra(
                                               45
14 dKp, dKm = dkrauses
                                                               array([1, s]), array([1, r])
                                               46
                                                          )/2
                                               47
16 # Plus state:
                                                          T_krauses.append(Tsr)
                                               48
17 plus = array([1, 1]) / sqrt(2)
                                               49 # If not provided derivative is by
                                               50 # default 0:
18 # Minus state:
19 minus = array([1, -1]) / sqrt(2)
                                                    = ParamChannel(
                                                      krauses=T_krauses, env_dim=2
21 # V_theta matrix:
                                               53 )
```

```
54

55 Lambda_tilde = Phi.link_env(T)

56 # or equivalently:

57 Lambda_tilde = Phi * T
```

When provided with env_dim argument, the constructor of ParamChannel will assume that the channel acts on a space $\mathcal{E} \otimes \mathcal{S}$ with dim \mathcal{E} given by the argument. All functions implementing MOP and ISS algorithms from Sec. 3.3 and Sec. 3.4 can take such a channel as their argument and optimize the corresponding QFI for a sequence of channels as in Fig. 7(A):

Bounds inthis case can be computed using ad_bounds_correlated and ad_asym_bounds_correlated. In contrast to the bounds for uncorrelated case these bounds are not necessarily tight asymptotically. They are computed by upper-bounding QFI for adaptive strategy where every m-th control operation has access to the environment, for some integer m. This leads to a leakage of information form the environment, which may make the bound less tight. Naturally, the bigger m makes the bound tighter but at the same time it exponentially increases the execution time. Realistically, one can compute the bound for $m \lesssim 5$ in case of qubit channels. An exemplary code to compute the bound is given below:

where ns = [1, 1 + m, 1 + 2m, ...,], bound= $[b_1, b_{1+m}, b_{1+2m}, ...]$ and b_n is an upper bound on

 $F_O^{(n)}(\Lambda_\theta)$.

Note, that the construction (50), (51) is not unique and correlations (49) can be modeled using different $\tilde{\Lambda}_{\theta}$. For example a quantum channel:

$$t: \mathcal{L}(\mathcal{E}) \ni \rho \mapsto \sum_{s,r} t_{sr} \rho \, t_{sr}^{\dagger} \in \mathcal{L}(\mathcal{E}),$$
$$t_{sr} = \sqrt{\frac{1 + sr\sqrt{c}}{2}} \, |s\rangle \langle r| \,, \quad (52)$$

satisfies $\mathbf{t} \circ \mathbf{t} = \mathbf{T}$ thus $\tilde{\Lambda}_{\theta} = \mathbf{t} * \Phi_{\theta} * \mathbf{t}$ will give the same $\Lambda_{\theta}^{(N)} = \tilde{\Lambda}_{\theta} * \dots * \tilde{\Lambda}_{\theta}$ as before. This observation is important for calculation of upper-bounds because of the aforementioned fact that they are not computed for the whole $\tilde{\Lambda}_{\theta}^{(N)}$ but for N/m blocks of size m and the construction influences how these blocks begin and end. For example, it turns out that the original construction (51) gives in this case an unrealistic HS and the optimal bound is achieved for (52), see [28] for more discussion.

Values of the QFI for anti-correlated (c=-0.75) dephasing case are shown in Figs.7 (B) and (C). Note, that the presence of (anti)correlations significantly increases the obtained QFI which becomes even larger then the upper-bounds for uncorrelated case. Interestingly, we can see that the adaptive strategy with $d_{\mathcal{A}}=2$ is optimal for $N \leq 5$, unlike in the uncorrelated dephasing case, see Fig. 6(B).

4 Advanced package usage—optimization of strategies with arbitrary structures

In addition to the functions presented in Sec. 3, QMetro++ allows the user to define their own strategy and then optimize it using the ISS algorithm. Strategies are defined via a straightforward-to-use symbolic programming. User creates a tensor network representing their strategy where some of the nodes are marked as constants and others are marked as variables to be optimized over—let us call their set \mathcal{V} . This strategy is then plugged into function <code>iss_opt</code> which based on the provided data constructs pre-QFI:

$$F(\mathcal{V}) = 2\operatorname{Tr}(\dot{\rho}_{\theta}\mathfrak{L}) - \operatorname{Tr}(\rho_{\theta}\mathfrak{L}^2),$$
 (53)

where ρ_{θ} and \mathfrak{L} are defined as in Fig. 9 and $\dot{\rho}_{\theta}$ is created from ρ_{θ} using the Leibniz (chain) rule.

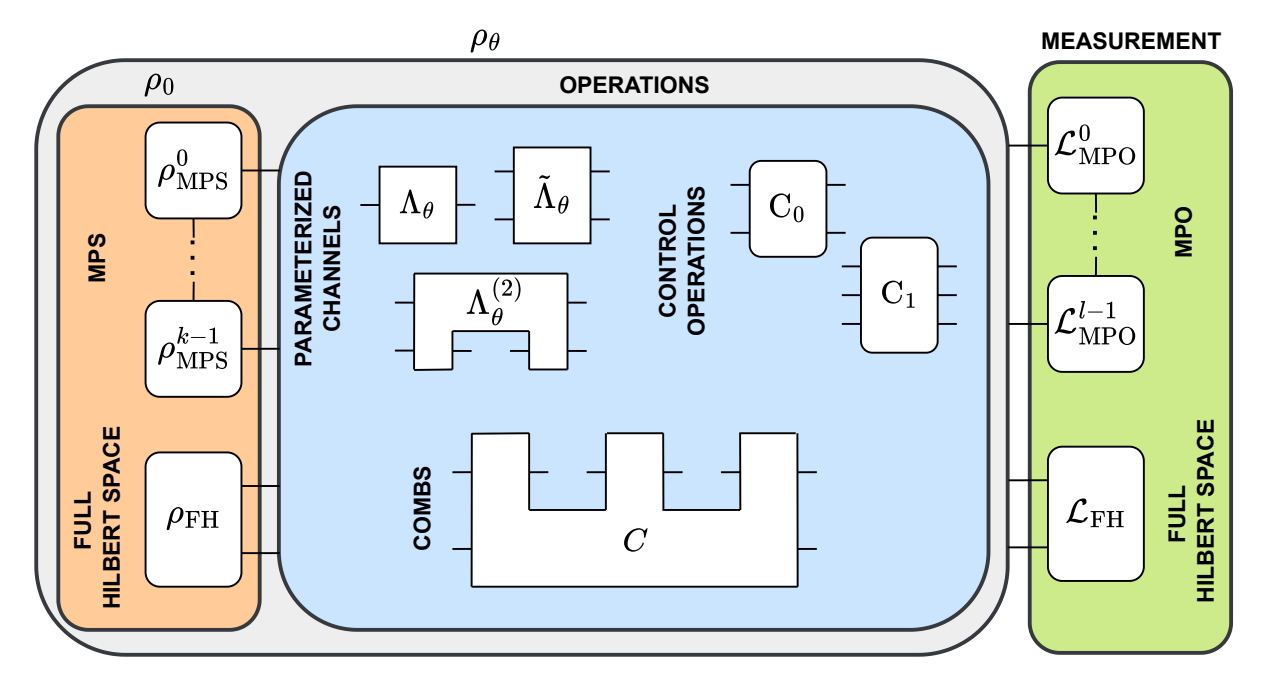


Figure 9: Diagram of strategy with arbitrary structure that can be optimized using iss_opt. Input state - ρ_0 might consist of MPSs and/or states on a full Hilbert. The input states goes through an arbitrary arrangement of parametrized channels, control operations and combs. The only requirements are that operations outputs are connected to operations inputs and that there are no cycles. Finally, the state obtained after application of each operation - ρ_θ is being measured. The measurement is specified by the form of the pre-SLD matrix $\mathfrak L$ which can be a MPO and/or a matrix on a full Hilbert space. States, control operations and combs can be marked as variable or constant, pre-SLD must be variable and parametrized channels must be constant.

Then the function optimizes the above pre-QFI over each variable node one by one in a typical ISS manner.

In Sec. 4.1 we explain the class of QMetro++ tensors (placed in qmtensor folder, see Fig. 2) which are the building blocks of strategies. Then in Sec. 4.2 we show how such strategy can be created using the example of collisional metrological model.

4.1 QMetro++ tensors

A general strategy in QMetro++ is created by defining it as a tensor network of:

- density matrices,
- elements of MPOs of density matrices, in particular density matrices of MPSs (see (34)),
- parameter encoding channels
- control operations,
- quantum combs,
- measurements,

• elements of measurement MPOs.

connected by their physical and bond spaces like in diagram in Fig. 9. Some input states, control operations, quantum combs and all measurements are marked as variables of the pre-QFI function (53) and they will be optimized by the ISS algorithm. Each non-measurement node is represented using their tensor representation (see detailed explanation in the Appendix B) and measurements are represented via a tensor representation of the pre-SLD matrix \mathfrak{L} .

In practice, this means that each node of the network has to be initialized as an object of QMetro++ tensor class (see Fig. 10). There are five kinds of tensor classes:

- GeneralTensor a class containing attributes and methods common to all tensors, such as the shape or the contraction operation. It is an abstract class [47] i.e. it is only a blueprint for other classes to inherit from and it is not meant to be used in any computations directly.
- ConstTensor a class representing tensors that stay constant during the optimization

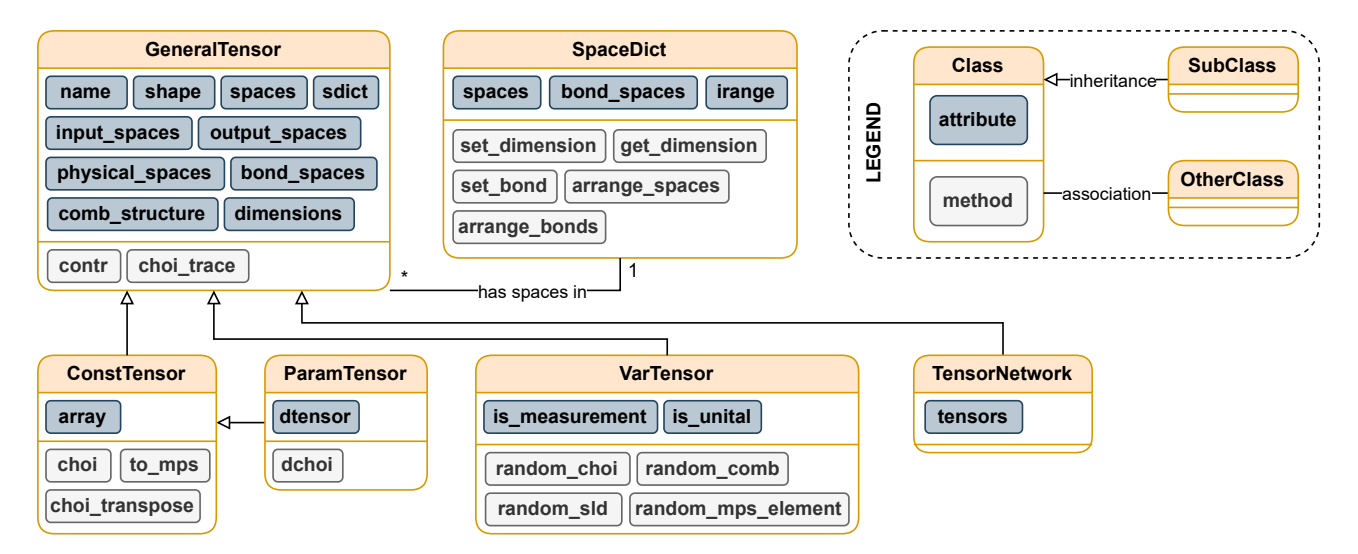


Figure 10: UML diagram of classes used for creation of strategies with their most important attributes and methods. Subclasses inherit all attributes and methods of their parent class. Instances of GeneralTensor and its subclasses can access a SpaceDict instance through their sdict attribute. Two tensors can be contracted with each other only when they have the same space dictionaries as sdict.

process.

- ParamTensor a subclass of ConstTensor which has an additional attribute defining its derivative over the measured parameter θ . It is meant to represent parameter encoding channels Λ_{θ} .
- VarTensor class of tensors which are being optimized by the ISS algorithm. Members of this class store information specifying how they should be initialized and optimized (for example that they are CPTP channels, quantum combs or pre-SLD matrices) but they do not have any value, that is they are only symbols.
- TensorNetwork networks of constant, parametrized and variable tensors.

Additionally, there is one more class, SpaceDict, that stores the information about the names, dimensions and types of the respective spaces. For example:

```
import numpy as np
from qmetro import *

sd = SpaceDict()
fmathraightarrow # Adding physical spaces with names
fmathraightarrow # 'a', 'b' and dimension 2 to sd.
fmathraightarrow # sd['a'] = 2
fmathraightarrow # Calling sd['a'] will return dimension
fmathraightarrow # Calling sd['a'] will return dimension
fmathraightarrow # fmath
```

```
12 print(sd['a']) # Prints 2.
13
14 # Adding bond space 'x':
15 sd.set_bond('x', 2)
16 print(sd['x']) # Prints 2.
17
18 # Accessing range of appropriate index:
19 print(sd.irange['a']) # Prints 4.
20 print(sd.irange['x']) # Prints 2.
```

Note that because physical index of a tensor representations of a CJ matrix is created by joining two indices related to the appropriate physical space its range is equal to the dimension of this space squared (see details in Appendix B).

Instances of tensors are created on spaces defined in the SpaceDict:

```
3 # Constant tensor can be initialized
4 # from a CJ matrix:
5 id_ab = np.identity(sd['a']*sd['b'])
6 ct0 = ConstTensor(
      ['a', 'b'], choi=id_ab, sdict=sd
10 # Its tensor representation is in array
11 # attribute:
12 ct0_ten_rep = ct0.array
13 # Order of its indices is in spaces
14 # attribute:
15 spaces = ct0.spaces
16
17 # Constant tensor can be initialized
18 # from its tensor representation
19 ct1 = ConstTensor(
      spaces, array=ct0_ten_rep, sdict=sd
21 )
```

```
22 # Parametrized tensor requires both its
24 # value and derivative. For example
25 # a tensor with trivial derivative will
26 # be:
27 zeros = np.zeros_like(id_ab)
28 pt = ParamTensor(
29 spaces, sdict=sd,
30 choi=id_ab, dchoi=zeros
31 )
```

Variable tensors require only spaces and their type is derived from additional attributes:

```
3 spaces = ['a', 'b']
4 \text{ bonds} = ['x']
6 # Variable tensor:
7 vt0 = VarTensor(spaces, sd)
9 # Types:
10 # > state:
11 vt1 = VarTensor(
      spaces, sd, output_spaces=spaces
12
13
14 # > element of density matrix of MPS:
15 vt1 = VarTensor(
      spaces + bonds, sd,
      output_spaces=spaces
17
18 )
19 # > CPTP map of a channel 'a'->'b':
20 vt1 = VarTensor(
      spaces, sd, output_spaces=['b']
21
22 )
23 # > pre-SLD:
24 vt2 = VarTensor(
      spaces, sd, is_measurement=True
26 )
_{27} # > element of pre-SLD MPO:
28 vt2 = VarTensor(
      spaces + bonds, sd,
30
      is_measurement=True
31
```

Tensors can be contracted using either contracted, function with the same name or the star '*' symbol:

```
1 from qmetro import *
2
3 ch = par_dephasing(0.75)
4 choi = ch.choi()
5
6 sd = SpaceDict()
7 spaces = ['a', 'b', 'c']
8 for space in spaces:
9    sd[space] = 2
10
11 ct0 = ConstTensor(['a', 'b'], choi, sd)
12 ct1 = ConstTensor(['b', 'c'], choi, sd)
13
14 # Contraction of 'b' space.
```

*	GT	СТ	PT	VT	TN
GT	Error	Error	Error	Error	Error
СТ	Error	CT	PT	TN	TN
PT	Error	PT	PT	TN	TN
VT	Error	TN	TN	TN	TN
TN	Error	TN	TN	TN	TN

Table 2: Type of a contraction result for various tensor pairs: GT-GeneralTensor, CT-ConstTensor, PT-ParamTensor, VT- VarTensor, TN-TensorNetwork. Contraction with generalized tensor raises an error because instances of this class are not meant to be used in calculations. When ParamTensor is contracted with a ConstTensor or a ParamTensor the derivative of the result is computed using the Leibnitz (chain) rule.

```
15 ct2 = ct0.contr(ct1)
16 # or equivalently
17 ct2 = contr(ct0, ct1)
18 # or equivalently
19 ct2 = ct0 * ct1
```

While contraction of two ConstTensors simply creates a new ConstTensor this is not the case when one of the contracted tensor is a VarTensor because it does not have any value. Contraction with a VarTensor creates a TensorNetwork consisting of the two tensors:

```
1 ...
2
3 ct = ConstTensor(['a', 'b'], choi, sd)
4 vt = VarTensor(['b', 'c'], sd)
5 # Tensor network of ct and vt connected
6 # by 'b' space:
7 tn = ct * vt
8
9 # Elements of tensor network can be
10 # accessed using tensor and name
11 # attributes:
12 print(tn.tensors[ct.name] is ct) # True.
13 print(tn.tensors[vt.name] is vt) # True.
```

Simmilarly, a contraction with a TensorNetwork creates another TensorNetwork. Results of all possible contraction combinations are presented in Table 2.

4.2 Collisional strategy

We will describe the creation of a custom strategy using the example of a *collisional strategy* depicted in Fig. 11(A). Physically, we can imagine this scheme to represent a situation where multiple-particles, potentially entangled with each other initially, approach one by one the

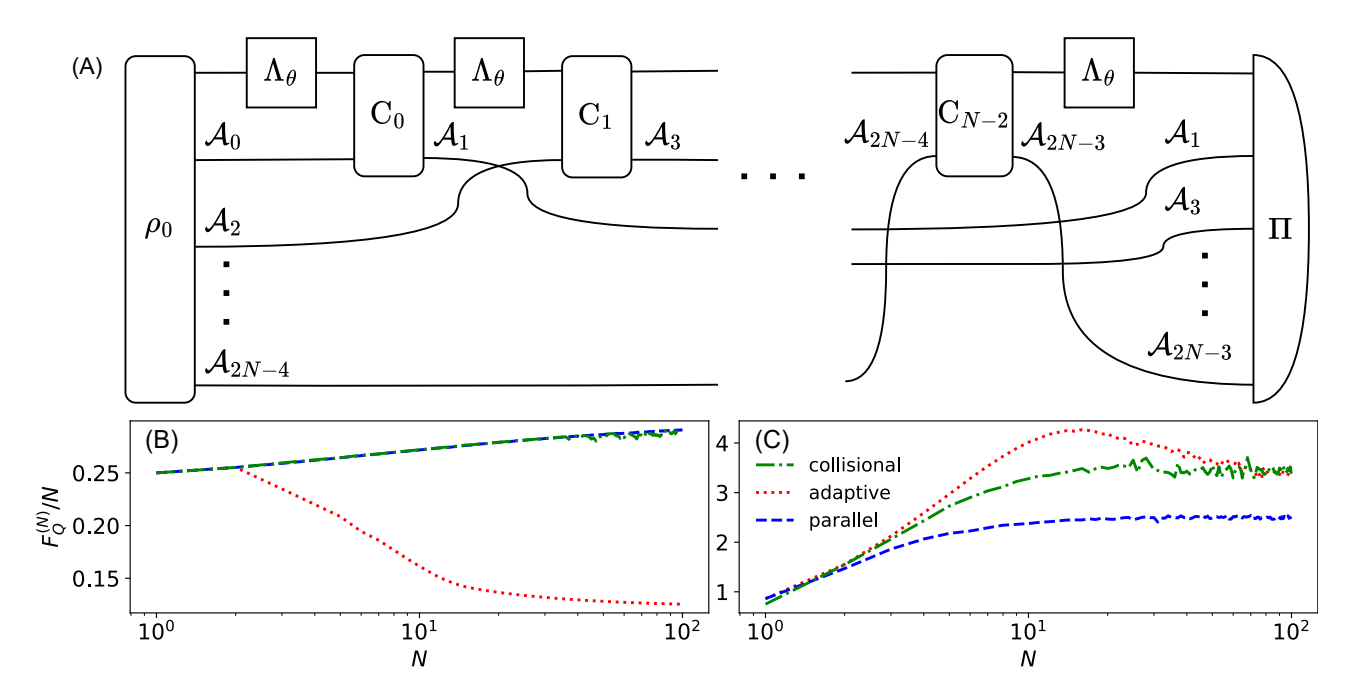


Figure 11: (A) Diagram of collisional strategy with multiple parametrized channels Λ_{θ} and ancillas \mathcal{A}_{i} . Values of QFI normalized by number of channel uses - N for: (B) dephasing (p=0.75) (C) amplitude damping (p=0.75) and different strategies: adaptive - with $d_{\mathcal{A}}=2$ - blue dashed line, parallel with $d_{\mathcal{A}}=2$, $r_{\mathrm{MPS}}=\sqrt{r_{\mathfrak{L}}}=2$ - red dotted line, collisional with $d_{\mathcal{A}}=2$, $r_{\mathrm{MPS}}=\sqrt{r_{\mathfrak{L}}}=2$ - green dash-dotted line.

sensing system with which they interact locally via control operations C_i , carrying away information about the parameter while at the same time causing some back-action on the sensing system itself.

This strategy may be viewed as a hybrid of parallel and adaptive strategy where each control operation C_i has their own ancilla which is measured immediately after the action of C_i . Notice, that if all C_i were put to SWAP gates one would regain the parallel strategy. On the other hand, this strategy does not allow control operations to communicate with each other like in the most general adaptive strategy. Therefore the QFI for this strategy must be at least as good as for the parallel strategy but in general will be worse than for the adaptive strategy with ancilla d_A^{N-1} , where d_A is dimension of a single ancillary system in the collisional strategy.

We can now create a tensor network representing the collisional strategy. In the following we will use functions from qmtensor/creators folder, see Fig. 2. These functions greatly simplify the process by creating the whole structures (for example the density matrix of an MPS) and they make the code more readable. Let us start by defining the necessary spaces:

```
1 from qmetro import *
```

```
3 # Number of parametrized channels:
4 N = 10
5 d_a = 2 # Ancilla dimension.
6
7 sd = SpaceDict()
8
9 # arrange_spaces will create a series of
10 # spaces ('INP', 0), ..., ('INP', N-1)
11 # with specified dimension and it will
12 # return a list of their names:
13 # > input spaces of parametrized
14 # channels:
15 inp = sd.arrange_spaces(N, 2, 'INP')
16 # > output spaces of parametrized
17 # channels:
18 out = sd.arrange_spaces(N, 2, 'OUT')
19 # > ancillas:
20 anc = sd.arrange_spaces(2*N-2, 2, 'ANC')
```

The input state can be created using input_state_var or mps_var_tnet:

Both of these functions create the same MPS but mps_var_tnet returns additionally names of its components and bond spaces which might become useful later for accessing the optimization results.

Tensors of parameter encoding channels can be created using tensor method from the ParamChannel class:

```
1 # Parameter encoding channel:
2 ch = par_dephasing(0.75)
4 # This will be the tensor network of our
5 # strategy:
6 \text{ tnet} = \text{rho0}
8 # Adding channels to tnet:
9 for i in range(N):
      inp_i = inp[i] # i-th input space.
       out_i = out[i] # i-th output space.
11
      pt = ch.tensor(
           [inp_i], [out_i], sdict=sd,
13
           name=f'CHANNEL{i}'
14
15
       tnet = tnet * pt
```

We want the control operations to be CPTP maps hence we will use cptp_var creator:

```
1 for i in range(N-1):
      # i-th control input spaces:
      c_inp = [out[i], anc[2*i]]
3
      # i-th control output spaces:
4
      c_out = [inp[i+1], anc[2*i+1]]
      # Variable control operation:
6
      vt = cptp_var(
          c_inp, c_out, sdict=sd,
          name=f'CONTROL{i}'
9
      )
10
      tnet = tnet * vt
11
```

Similarly, as in the case of the input state, the measurement can be created in one of two ways:

In summary, the code is:

```
1 from qmetro import *
3 ch = par_dephasing(0.75) # Channel.
 _4 N = 10 # Number of channels.
5 d_a = 2 \# Ancilla dimension.
6 \text{ r_mps} = 2 \text{ # MPS bond dimension.}
7 r_L = r_mps**2 \# pre-SLD bond dimension.
9 sd = SpaceDict()
inp = sd.arrange_spaces(N, 2, 'INP')
11 out = sd.arrange_spaces(N, 2, 'OUT')
12 anc = sd.arrange_spaces(2*N-2, 2, 'ANC')
14 rho0_spaces = [inp[0]] + anc[::2]
15 rho0, rho0_names, rho0_bonds =
      mps_var_tnet(rho0_spaces, 'RHOO', sd,
       r_mps)
16
17 \text{ tnet} = \text{rho0}
18 for i in range(N):
19
       pt = ch.tensor(
           [inp[i]], [out[i]], sdict=sd,
20
21
           name=f'CHANNEL{i}'
      )
       tnet = tnet * pt
25 for i in range(N-1):
       vt = cptp_var(
26
           [out[i], anc[2*i]],
27
           [inp[i+1], anc[2*i+1]],
28
           sdict=sd, name=f'CONTROL{i}'
       tnet = tnet * vt
31
33 spaces = anc[1::2] + [out[-1]]
34 Pi, Pi_names, Pi_bonds =
      mpo_measure_var_tnet(spaces, 'Pi', sd
      , r_L)
35
```

To optimize our strategy we need to simply put it into iss_opt function:

```
1 qfi, qfis, tn_opt, status = iss_opt(tn)
```

tnet = tnet * Pi

where qfi is the optimized QFI, qfis is pre-QFI value per iteration, status tells whether the optimization converged successfully and tn_opt is a copy of tn where each VarTensor is replaced with a ConstTensor storing the result of strategy optimization. To access those values we need to use the names of the required tensor and its spaces:

1 i = 2

```
3 # Accessing Choi matrix of the i-th
4 # channel:
5 name = f'CONTROL{i}'
  # i-th control operation tensor:
  C_i = tn_opt.tensors[name]
  spaces = [
      inp[i+1], anc[2*i+1], out[i],
      anc[2*i]
11
12
  # CJ matrix with spaces in the order
13
14 # given by the argument:
15 choi = C_i.choi(spaces)
  # Accessing MPS density matrix
  # i-th element:
19 name = rho0_names[i]
  # i-th element of the state's
21 # density MPO:
22 rho0_i = tn_opt.tensors[name]
2.3
24 \text{ spaces} = [
      rho0_bonds[i-1], rho0_spaces[i],
25
      rho0_bonds[i]
26
27
28 # MPS element with indices in the order
29 # given by the argument:
30 psi_i = rho0_i.to_mps(spaces)
```

Figs. 11 (B) and (C) show the optimized values of the QFI for collisional strategy together with the parallel and adaptive ones for comparison. It turns out that in case of the dephasing noise (B), additional control operations do not help and the results are the same as for the parallel strategy. On the other hand, for the amplitude damping noise (C) the collisional strategy is significantly better than the parallel one and appears to be able to beat the adaptive strategy for N > 100, under given limited ancillary dimension sizes. This proves that in this case, the optimal strategy found is qualitatively different from both the parallel and the adaptive ones.

5 Summary

We hope that the presented package will serve as an indispensable tool for anyone, who wants to identify optimal protocols in noise metrology scenarios as well as for those who want to compare the performance of strategies of particular structure with fundamental bounds.

While the package is at the moment focused solely on the single parameter QFI optimization paradigm, it may be in principle developed further to cover Bayesian as well as multi-parameter

frameworks. In case of Bayesian framework, though, we do not expect tensor-network methods to work as efficiently as in the QFI case. This is mainly due to the need to use larger ancilla spaces to effectively feed-forward information which is systematically increasing with the growing protocol length, see [22] for more discussion. This would limit applicability of these methods to small scale problems only, and go against the main purpose of this package, which is to provide numerical methods that work efficiently for large-scale quantum metrology problems. people interested in small-scale Bayesian estimation problems, we can recommend the QuanEstimation package [48], where implementation of some of quantum Bayesian estimation methods can be found.

In general, QuanEstimation package may be regarded as largely complementary to the present It provides a wider set of quantum estimation tools, combining both QFI-based and Bayesian methods. The package also has numerous tools dedicated to analyzing and optimizing experimentally relevant quantum control frameworks, as well as some multi-parameter quantum estimation tools. QuanEstimation has optimization procedures that allow to optimize input states in a basic single quantum channel estimation problem, as well as optimize adaptive strategies, with some predefined control structures. This said, efficiency of the proposed algorithms is limited to small scale problems, and even in this case, the optimization procedures employed do not guarantee that the result obtained is indeed optimal.

In case of multi-parameter estimation strategies, one may generalize the ISS and tensor-network methods in a rather straightforward way to optimize the trace of the QFI matrix, as in [49]. However, despite some novel works on this topic [50], a rigorous and at the same time numerically effective optimization of multi-parameter cost that could be applied to study the performance of noisy metrological protocols in the large N limit seems to be out of reach at this moment.

Finally, we should also mention, that we have independently studied and developed similar methods to study the channel discrimination problem [51], results of which will be reported elsewhere.

Acknowledgments. We thank Krzysztof

Chabuda for fruitful discussions regarding the inner workings of the TNQMetro package. This work has been supported by the "Quantum Optical Technologies" (FENG.02.01-IP.05-0017/23) project, carried out within the Measure 2.1 International Research Agendas programme of the Foundation for Polish Science co-financed by the European Union under the European Funds for Smart Economy 2021-2027 (FENG), as well as National Science Center (Poland) grant No.2020/37/B/ST2/02134.

References

- [1] Vittorio Giovannetti, Seth Lloyd, and Lorenzo Maccone. "Quantum metrology". Phys. Rev. Lett. **96**, 010401 (2006).
- [2] Geza Toth and Iagoba Apellaniz. "Quantum metrology from a quantum information science perspective". J. Phys. A: Math. Theor. 47, 424006 (2014).
- [3] Luca Pezzè, Augusto Smerzi, Markus K. Oberthaler, Roman Schmied, and Philipp Treutlein. "Quantum metrology with non-classical states of atomic ensembles". Rev. Mod. Phys. 90, 035005 (2018).
- [4] Emanuele Polino, Mauro Valeri, Nicolò Spagnolo, and Fabio Sciarrino. "Photonic quantum metrology". AVS Quantum Science 2, 024703 (2020).
- [5] David S. Simon. "Introduction to quantum science and technology". Springer Nature Switzerland. (2025).
- [6] R. Schnabel. "Squeezed states of light and their applications in laser interferometers". Physics Reports **684**, 1 51 (2017).
- [7] D. et al. Ganapathy. "Broadband quantum enhancement of the ligo detectors with frequency-dependent squeezing". Phys. Rev. X 13, 041021 (2023).
- [8] Charikleia Troullinou, Vito Giovanni Lucivero, and Morgan W. Mitchell. "Quantum-enhanced magnetometry at optimal number density". Phys. Rev. Lett. 131, 133602 (2023).
- [9] Christophe Cassens, Bernd Meyer-Hoppe, Ernst Rasel, and Carsten Klempt. "Entanglement-enhanced atomic gravimeter". Phys. Rev. X 15, 011029 (2025).
- [10] Edwin Pedrozo-Peñafiel, Simone Colombo, Chi Shu, Albert F. Adiyatullin, Zeyang

- Li, Enrique Mendez, Boris Braverman, Akio Kawasaki, Daisuke Akamatsu, Yanhong Xiao, and Vladan Vuletić. "Entanglement on an optical atomic-clock transition". Nature **588**, 414–418 (2020).
- [11] B. M. Escher, R. L. de Matos Filho, and L. Davidovich. "General framework for estimating the ultimate precision limit in noisy quantum-enhanced metrology". Nature Phys. 7, 406–411 (2011).
- [12] Rafał Demkowicz-Dobrzański, Jan Kołodyński, and Mădălin Guţă. "The elusive Heisenberg limit in quantumenhanced metrology". Nat. Commun. 3, 1063 (2012). arXiv:1201.3940.
- [13] Rafal Demkowicz-Dobrzański and Lorenzo Maccone. "Using entanglement against noise in quantum metrology". Phys. Rev. Lett. 113, 250801 (2014).
- [14] Rafal Demkowicz-Dobrzański, Marcin Jarzyna, and Jan Kołodyński. "Chapter four - quantum limits in optical interferometry". In E. Wolf, editor, Progress in Optics. Volume 60 of Progress in Optics, pages 345–435. Elsevier (2015).
- [15] Rafał Demkowicz-Dobrzański, Jan Czajkowski, and Pavel Sekatski. "Adaptive quantum metrology under general markovian noise". Phys. Rev. X 7, 041009 (2017).
- [16] Sisi Zhou, Mengzhen Zhang, John Preskill, and Liang Jiang. "Achieving the heisenberg limit in quantum metrology using quantum error correction". Nature Communications 9, 78 (2018).
- [17] Krzysztof Chabuda, Jacek Dziarmaga, Tobias J. Osborne, and Rafal Demkowicz-Dobrzanski. "Tensor-network approach for quantum metrology in many-body quantum systems". Nature Communications 11, 250 (2020).
- [18] Sisi Zhou and Liang Jiang. "Asymptotic theory of quantum channel estimation". PRX Quantum 2, 010343 (2021).
- [19] Anian Altherr and Yuxiang Yang. "Quantum metrology for non-markovian processes". Phys. Rev. Lett. **127**, 060501 (2021).
- [20] Qiushi Liu, Zihao Hu, Haidong Yuan, and Yuxiang Yang. "Optimal strategies of quantum metrology with a strict hierarchy". Phys. Rev. Lett. 130, 070803 (2023).

- [21] Stanisław Kurdziałek, Wojciech Górecki, Francesco Albarelli, and Rafał Demkowicz-Dobrzański. "Using adaptiveness and causal superpositions against noise in quantum metrology". Phys. Rev. Lett. 131, 090801 (2023).
- [22] Stanisław Kurdziałek, Piotr Dulian, Joanna Majsak, Sagnik Chakraborty, and Rafał Demkowicz-Dobrzański. "Quantum metrology using quantum combs and tensor network formalism". New Journal of Physics 27, 013019 (2025).
- [23] Qiushi Liu and Yuxiang Yang. "Efficient tensor networks for control-enhanced quantum metrology". Quantum 8, 1571 (2024).
- [24] C. W. Helstrom. "Quantum detection and estimation theory". Academic press. (1976).
- [25] Samuel L. Braunstein and Carlton M. Caves. "Statistical distance and the geometry of quantum states". Phys. Rev. Lett. 72, 3439– 3443 (1994).
- [26] Mattteo G. A. Paris. "Quantum estimation for quantum technologies". International Journal of Quantum Information 07, 125– 137 (2009).
- [27] Krzysztof Chabuda and Rafał Demkowicz-Dobrzański. "Tnqmetro: Tensor-network based package for efficient quantum metrology computations". Computer Physics Communications 274, 108282 (2022).
- [28] Stanislaw Kurdzialek, Francesco Albarelli, and Rafal Demkowicz-Dobrzanski. "Universal bounds for quantum metrology in the presence of correlated noise" (2024). arXiv:2410.01881.
- [29] Piotr Dulian and Stanisław Kurdziałek. "Python optimization package for large scale quantum metrology with customized strategy structures". GitHub repository (2025). url: https://github.com/pdulian/qmetro.
- [30] Akio Fujiwara. "Quantum channel identification problem". Phys. Rev. A 63, 042304 (2001).
- [31] Jan Kołodyński and Rafał Demkowicz-Dobrzański. "Efficient tools for quantum metrology with uncorrelated noise". New Journal of Physics 15, 073043 (2013).
- [32] Masahito Hayashi. "Comparison between the cramer-rao and the mini-max approaches in quantum channel estimation".

- Communications in Mathematical Physics **304**, 689–709 (2011).
- [33] Johannes Jakob Meyer, Sumeet Khatri, Daniel Stilck França, Jens Eisert, and Philippe Faist. "Quantum metrology in the finite-sample regime" (2023). arXiv:2307.06370.
- [34] Rafał Demkowicz-Dobrzański, Wojciech Górecki, and Mădălin Guţă. "Multiparameter estimation beyond quantum fisher information". Journal of Physics A: Mathematical and Theoretical 53, 363001 (2020).
- [35] S. M. Kay. "Fundamentals of statistical signal processing: Estimation theory". Signal processing series. Prentice Hall. (1993).
- [36] Giulio Chiribella, Giacomo Mauro D'Ariano, and Paolo Perinotti. "Theoretical framework for quantum networks". Phys. Rev. A 80, 022339 (2009).
- [37] Akio Fujiwara and Hiroshi Imai. "A fibre bundle over manifolds of quantum channels and its application to quantum statistics". J. Phys. A 41, 255304 (2008).
- [38] Ingemar Bengtsson and Karol Zyczkowski. "Geometry of quantum states: an introduction to quantum entanglement". Cambridge University Press. (2006).
- [39] MOSEK ApS. "The mosek optimization toolbox for python manual. version 10.2.". (2024). url: http://docs.mosek.com/latest/pythonapi/index.html.
- [40] Rafał Demkowicz-Dobrzański. "Optimal phase estimation with arbitrary a priori knowledge". Phys. Rev. A 83, 061802 (2011).
- [41] Katarzyna Macieszczak. "Quantum Fisher Information: Variational principle and simple iterative algorithm for its efficient computation" (2013). arXiv:1312.1356.
- [42] Katarzyna Macieszczak, Martin Fraas, and Rafał Demkowicz-Dobrzański. "Bayesian quantum frequency estimation in presence of collective dephasing". New Journal of Physics 16, 113002 (2014).
- [43] Géza Tóth and Tamás Vértesi. "Quantum states with a positive partial transpose are useful for metrology". Phys. Rev. Lett. **120**, 020506 (2018).
- [44] Árpád Lukács, Róbert Trényi, Tamás Vértesi, and Géza Tóth. "Optimiza-

- tion in quantum metrology and entanglement theory using semidefinite programming" (2022). arXiv:2206.02820.
- [45] Jacob C Bridgeman and Christopher T Chubb. "Hand-waving and interpretive dance: an introductory course on tensor networks". Journal of Physics A: Mathematical and Theoretical **50**, 223001 (2017).
- [46] Ulrich Schollwöck. "The density-matrix renormalization group in the age of matrix product states". Annals of Physics **326**, 96 192 (2011).
- [47] Joshua Bloch. "Effective java: Programming language guide". Addison-Wesley. (2018).
- [48] Mao Zhang, Huai-Ming Yu, Haidong Yuan, Xiaoguang Wang, Rafał Demkowicz-Dobrzański, and Jing Liu. "Quanestimation: An open-source toolkit for quantum parameter estimation". Phys. Rev. Res. 4, 043057 (2022).
- [49] Francesco Albarelli and Rafał Demkowicz-Dobrzański. "Probe incompatibility in multiparameter noisy quantum metrology". Phys. Rev. X 12, 011039 (2022).
- [50] Masahito Hayashi and Yingkai Ouyang. "Finding the optimal probe state for multiparameter quantum metrology using conic programming". npj Quantum Information 10 (2024).
- [51] Jessica Bavaresco, Mio Murao, and Marco Túlio Quintino. "Strict hierarchy between parallel, sequential, and indefinite-causal-order strategies for channel discrimination". Physical Review Letters 127 (2021).

A Choi-Jamiołkowski matrix and the link product

When discussing networks of channels it is useful to use a notion of the *Choi-Jamiołkowski matrix* (CJ). For a linear map

$$P: \mathcal{L}(\mathcal{A}) \mapsto \mathcal{L}(\mathcal{B}),$$
 (54)

its CJ matrix is given by [36, 38]:

$$P = (P \otimes \mathbb{I}_{\mathcal{A}}) (|\Phi\rangle\langle\Phi|) \in \mathcal{L} (\mathcal{B} \otimes \mathcal{A}), \qquad (55)$$

where $|\Phi\rangle = \sum_i |i\rangle \otimes |i\rangle$ is a non-normalized maximally entangled state on $\mathcal{A} \otimes \mathcal{A}$. In what follows, CJ matrices of maps (e.g. map P) will be denoted with the same symbol but in italics (e.g. P). CJ matrix P has many useful properties [38]:

Fact A.1 (CJ operator properties) For a map P from (54) and its CJ matrix defined by formula (55) the following properties are satisfied:

- 1. if P represents a state preparation procedure then P is the density matrix of the state it produces,
- 2. if $P = Tr_A$ represents tracing out over the space A than P is the identity matrix on A,
- 3. P is completely positive if and only if P is positive semidefinite,
- 4. P is trace-preserving if and only if $\operatorname{Tr}_{\mathcal{B}}P = \mathbb{1}_{\mathcal{A}}$,
- 5. P is unital that is $P(\mathbb{1}_{\mathcal{A}}) = \mathbb{1}_{\mathcal{B}}$ if and only if $\operatorname{Tr}_{\mathcal{A}}P = \mathbb{1}_{\mathcal{B}}$.

Additionally, for two maps:

$$P: \mathcal{L}(\mathcal{H}_0) \mapsto \mathcal{L}(\mathcal{H}_1 \otimes \mathcal{H}_2), \qquad (56)$$

$$Q: \mathcal{L}(\mathcal{H}_2 \otimes \mathcal{H}_3) \mapsto \mathcal{L}(\mathcal{H}_4),$$

the CJ matrix of their composition R:

is the link product of P and Q:

$$R = P * Q = \operatorname{Tr}_2 \left[\left(\mathbb{1}_{34} \otimes P^{T_2} \right) \left(Q \otimes \mathbb{1}_{01} \right) \right], (58)$$

where $\mathbb{1}_{ij}$, Tr_{ij} and T_i denote identity, partial trace and partial transposition on $\mathcal{H}_i \otimes \mathcal{H}_j$ and

 \mathcal{H}_i . In case of CJ matrices acting on more complicated Hilbert spaces for example:

$$M \in \mathcal{L}\left(\bigotimes_{i \in X} \mathcal{H}_i\right), \quad N \in \mathcal{L}\left(\bigotimes_{i \in Y} \mathcal{H}_i\right), \quad (59)$$

where X and Y are some sets of indices, the link product is

$$M * N =$$

$$= \operatorname{Tr}_{X \cap Y} \left[\left(\mathbb{1}_{Y \setminus X} \otimes M^{T_{X \cap Y}} \right) \left(N \otimes \mathbb{1}_{X \setminus Y} \right) \right],$$

where Tr_Z , $\mathbb{1}_Z$ and T_Z are trace, identity matrix and transposition for $\bigotimes_{i \in Z} \mathcal{H}_i$ and it is assumed that there are SWAP operators put inside the trace such that terms in round brackets act on the tensor product of spaces \mathcal{H}_i in the same order. Additionally, since the relation between channels and CJ matrices is isomorphic [36, 38] link product can be naturally extended to channels.

B Tensor network formalism and tensor representation

It is convenient to denote tensors and their contractions using diagrams. In this formalism tensor $T^{\mu_0\mu_1...\mu_{n-1}}$ is represented as a vertex of a graph with edge for each index:

$$T^{\mu_0\mu_1\dots\mu_{n-1}} = \begin{array}{c} \mu_{n-1} \\ \mu_{n-2} \end{array} \qquad \begin{array}{c} \mu_0 \\ \mu_1 \\ \end{array} \qquad (61)$$

and contraction of indices is depicted as a connection of these edges:

$$V^{\mu\nu}W^{\nu\eta} = -\frac{\mu}{V} V - \frac{\nu}{W} \frac{\eta}{\eta} . \tag{62}$$

Tensor network formalism can be used to conveniently express link product. For a Hilbert space $\mathcal{H} = \bigotimes_{i=0}^{n-1} \mathcal{H}_i$ with $d_i := \dim \mathcal{H}_i$ and a linear operator acting on it:

$$M = \sum_{\substack{a_0, \dots, a_{n-1} \\ b_0, \dots, b_{n-1}}} M_{b_0 \dots b_{n-1}}^{a_0 \dots a_{n-1}} |a_0 \dots a_{n-1}\rangle \langle b_0 \dots b_{n-1}|,$$
(63)

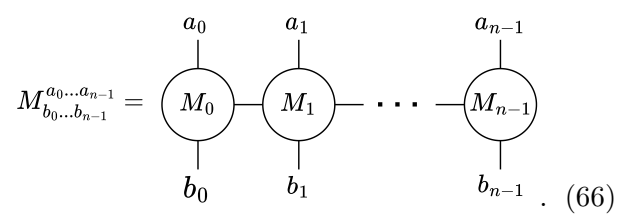
we define $tensor\ representation$ of M to be a tensor:

$$\tilde{M}^{x_0...x_{n-1}} = M^{a_0...a_{n-1}}_{b_0...b_{n-1}}$$
 for $x_i = d_i a_i + b_i$. (64)

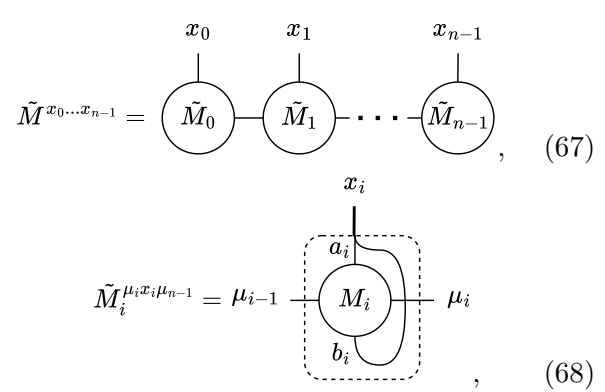
Next, consider channels P, Q and R = P * Q from (56) and (57). One can easily check that tensor representations of their CJ matrices satisfy:

which mirrors the circuit diagram from (57). Due to the similarity of these two diagrams, in the main text we drop the symbol \sim and we depict strategies using circuit diagrams and tensor network diagrams interchangeably.

In case M is a MPO:



we can extend this definition to its components M_i such that \tilde{M} will be a result of contraction of tensors \tilde{M}_i :



that is only physical indices of M_i are joined. This combined with the use of '*' to denote both link product and tensor contraction allows for convenient depiction of link product with CJ matrices which are MPOs.

List of acronyms

CCR Classical Cramér-Rao

CFI Classical Fisher Information

CJ Choi-Jamiołkowski

CPTP Completely Positive Trace Preserving

HS Heisenberg Scaling

ISS Iterative See-Saw

MOP Minimization Over Purifications

MPO Matrix Product Operator

MPS Matrix Product State

QCR Quantum Cramér-Rao bound

SDP Semidefinite programming

SS Standard Scaling

SLD Symmetric Logarithmic Derivative

QFI Quantum Fisher Information

UML Unified Modeling Language